Image Reconstruction in Functional Optical Neuroimaging
The modelling and separation of the scalp blood flow: A research proposal

Javier Herrera-Vega, Felipe Orihuela-Espina

Technical Report No. CCC-15-002
March 26, 2015

Department of Computational Sciences

National Institute for Astrophysics Optics and Electronics
Tonantzintla, Puebla, México

Abstract

Optical imaging is an emerging modality to image biological tissue non-invasively. Its use for brain imaging function is known as functional Near Infrared Spectroscopy (fNIRS). Its use as a functional neuroimaging modality demands attending numerous factors many which are still being investigated. One of these factors is the image reconstruction, particularly critical for brain understanding. The main problem to investigate in this research is the inherent inverse problem of the optical neuroimage reconstruction in which several sources of noise exist aggravating the ill-posed nature of the problem. Popular methods address this problem with strong assumptions leading to a reconstruction departing from reality. In order to alleviate this situation, this research, aims to develop a reconstruction based on a precise model of the forward problem, the quantification of the noise due to the blood irrigation in the scalp as one of the leading artefacts affecting reconstruction and the use of this information as an *a priori* knowledge in order to improve reconstruction. The main scientific contributions will be; the better understanding of the image formation process in the optical neuroimage domain, the more accurate forward model developed, the quantification of noise from scalp irrigation and the solution to the inverse problem informed with the *a priory* knowledge. Preliminary results shows that reconstruction is more viable when the source of noise is avoided.

Keywords

Image reconstruction, inverse problem, fNIRS, neuroimage

Contents

List of Figures

List of Tables

List of acronyms

fNIRS functional Near Infrared Spectroscopy

SNR Signal to Noise Ratio

SID Spectral Intensity Distribution

DOI Diffuse Optical Imaging

BLL Beer-Lambert Law

MBLL Modified Beer-Lamber Law

HBO$_2$ Oxyhaemoglobin

HHb Deoxyhaemoglobin

rCMRO$_2$ region Cerebral Metabolic Rate of Oxygen

rCBF region Cerebral Blood Flow

rCBV region Cerebral Blood Volume

CSF Cerebrospinal fluid

BOLD Blood-oxygen-level dependent

fMRI functional Magnetic Resonance Imaging

DPF Differential Path-length Factor

OD Optical Density

RTE Radiative Transfer Equation

FEM Finite Element Method

MC Monte Carlo

RW Random Walks

GPU Graphics Processor Unit

SAC Specific Absorption Coefficient

HWHM Half Width at Half Maximum

DMRF Discrete Markov Random Field

1 Introduction

Diffuse optical neuroimaging commonly known as functional Near Infrared Spectroscopy (fNIRS) is a neuroimage modality that permits interrogating brain activity non invasively (Villringer & Chance, 1997; Strangman *et al.*, 2002). Its working principle involves irradiating infrared light at the subject's scalp, this light propagates through the tissue and eventually part of it is backscattered to the surface where it is collected by a photodetector. The sensed attenuated light encodes information about brain activity consequence of the alterations in absorption and scattering induced as a result of physiological changes associated to such activity, mainly brain haemodynamics.

The reconstruction of the diffuse optical image is the transformation of the exiting radiation intensity captured by the photodetectors into quantified physiological information of interest, and specifically, in optical neuroimaging the estimation of haemodynamic changes from attenuation Arridge & Schotland (2009); Scholkmann *et al.* (2014).

One of the most interfering elements to obtain a reliable reconstruction is blood irrigation to scalp which is widely accepted as one of the main sources of noise in fNIRS (Haeussinger *et al.*, 2011; Takahashi *et al.*, 2011; Tachtsidis *et al.*, 2010). In order to alleviate its effect in recovering brain haemodynamics as a proxy of brain activity, a number of solutions have been already proposed in literature including having a proximal channel to sense shallow attenuation (multidistance optode arrays), concurrent observations with Doppler or exploitation of transients but they are still under discussion by the community (Kirilina *et al.*, 2013).

As it will be described in this proposal, in computational terms the above represent an unresolved challenge in the form of an strongly non-linear inverse problem with the further complexity of being ill-posed which is often dealt with by means of aggressive regularization. Briefly the image reconstruction is a back projection from a low dimensional image space where points in this space represent pixel intensities to a higher dimensional space of histophysiological parameters where points represent tissue composition. Importantly the analytical form of the accompanying forward projection is unknown. The noise added by skin blood flow deforms the forward mapping in a non-linear manner further stressing the degeneracy of the Jacobian determinant. Removal of this noise source can be computationally addressed by blind source separation but this approach has thus far fall short. The inclusion of constraints to the regularized reconstruction in the form of prior seems an appealing alternative scarcely explored.

Several reasons might help to explain the difficulty to circumvent the problem including the need of a more complex hardware, the stimulus-locked component of such irrigation, or the lack of forward models explicitly incorporating the contribution of the scalp blood irrigation.

1.1 Motivation

Many of the factors affecting the optical signal encoding the brain haemodynamics are widely recognised, yet surprisingly poorly understood (Orihuela-Espina *et al.*, 2010) with the paradigmatic case being the physiological noise including scalp irrigation. Indeed, Kirilina *et al.* (2013) remarks that the precise physiological fNIRS noise mechanisms are unknown. Notwithstanding, it is well known that scalp haemodynamics obfuscates brain haemodynamics (Tachtsidis *et al.*, 2010), and that its privileged location near the surface in the optical path augments its disturbance over the signal of interest perhaps representing as much as 76% of the attenuation (Scholkmann *et al.*, 2014). Yet understanding of this component of the systemic noise remains incomplete. For instance, time variation of the skin blood flow signal might be task evoked (Kohno *et al.*, 2007) but even its task independent contribution to the fNIRS signal remains largely unexplored. Notwithstanding a number of efforts have been made to eliminate this contribution to the optical signal none yet definitive(Kirilina *et al.*, 2013). This gap in the knowledge demands attention.

Removal of the extracerebral systemics e.g. skin blood flow/volume, from the fNIRS signal requires accurate characterization of the quantification of the contribution of scalp haemodynamics to the remitted spectra. The model by Takahashi *et al.* (2011) only intended to confirm that most photons travelled through the scalp layer at optode separations that ranged from 5 to 30 mm. Moreover this noise contributes to the non-monotonic spectral observations, thus confusing the determinant of the Jacobian and hindering reconstruction. Computational solutions to this inverse problem like feeding prior knowledge to the regularization might succeed where instrumental e.g. short channel, exploitation of transients e.g. task-evoked differences, and concurrent recordings e.g. Doppler, have thus far prove insufficient.

1.2 Justification

Brain understanding is one the most important challenges currently faced by science Sporns (2010), and the BRAIN initiative with its investment surpassing $300 million USD is an excellent example of its importance. Neuroimages are our most direct way to interrogate the brain *in-vivo* along with psychological and psychophysical studies, and the only way to observe its function non-invasively. A number of neuroimages modalities are at the disposal of neuroscientists each one offering different views of the brain. fNIRS with its current tradeoff between spatial and temporal resolution, and its capability to achieve ecological validity in difficult experimental tasks is emerging as a dependable neuroimaging alternative in the study of neurodevelopment, psychiatric conditions or stroke among others (Boas *et al.*, 2014). The reconstruction of the brain haemodynamics from the diffuse optical signal is a complex inverse problem(Dehghani *et al.*, 2009b).

Inverse problems are an important issue in many fields of science Wang *et al.* (2011). In these problems both the forward projection (physical observation) and the backward

restoration (parameter retrieval) have to be properly understood to achieve the most faithful reconstruction. In optical neuroimaging, providing new solutions to the inverse problem e.g. perhaps by modeling certain unattended constraints, produces new knowledge that helps to improve the quality of the optical signal and more importantly, the brain function estimate as well. The development of computational methods to achieve a clearer image of the neural activity is important for:

- boost reliability of the optical neuroimaging technology

- permit more complex interrogation of the brain activity and in consequence benefitting research in neuroscience and

- alleviate operational constraints, perhaps opening the door to new applications e.g. clinical.

The main goal of this research is on one hand to establish the effect over the remitted spectra of the haemoglobin species present in the scalp and affecting the optical signal, and on the other hand, the development of computational solutions to alleviate its effect, and in consequence achieving a cleaner (less noisy) reconstruction of the markers of neural activity.

1.3   Frame and assessment

This thesis is framed in the project "CONACYT basic science: funtional Near Infrared Spectroscopy exploring the brain *in-vivo in-situ*, CONACYT-CB-2011-01-169558".

Despite the multidisciplinary nature of the thesis topic, which involves knowledge related to: optics, histophysiology, neuroscience and mathematics this work focus on computational solution to the reconstruction problem of the optical neuroimage. This research will be focus on the development of algorithms that permits inversion of the problem bounded by the histophysiological parameters of interest.

1.4   Specific problems to address

Specifically, this thesis aims at addressing the following three factors:

- The establishment of a computational forward model of transport radiation of the human adult head with a geometry and histophysiology as realistic as possible surpassing current models in faithfulness so that estimation of diffuse reflectance at tissue surface is enhanced. Critically this model will explicitly incorporate blood irrigation to scalp.

- The quantification of the non-linear contribution to the diffuse reflectance of the absorption due to the presence of the oxygenated and reduced haemoglobin species both due to normal irrigation as part of the global systemics and locally due to task evoked changes.

- Proposing a new approximation to the inverse and ill-posed reconstruction problem that considers a priori knowledge of the aforementioned quantification of scalp irrigation.

The former two further research aspects of the image formation process yet poorly investigated, whereas the latter offers a novel alternative for the reconstruction itself. Quantification of the attenuation due to the haemoglobin within the scalp open the door to remove its effect from the optical signal and hence permitting an image of better quality free from such noise.

As a collateral task, during this thesis, the contribution of several others histophysiological parameters, in addition to those related to scalp irrigation will be further scrutinized and questioned about their individual contribution to the final remitted spectra, and importantly which may strongly affect inversion. The rationale behind this more exhaustive parameter evaluation is to establish an inversion strategy guaranteeing the uniqueness of the mapping, as well as the stability of it by means of a regularization approach that incorporates a priori physiological information.

1.5 Contributions

The main contributions of this research are expected to be the following:

- A better understanding of the diffuse optical neuroimage formation process through the assessment of the contribution to the final remitted spectra of a set of histophysiological parameters, that is the forward mapping.

- The specific quantification of the attenuation introduced by blood irrigation to the scalp within histologically plausible ranges, that is one source of non-linearity of the problem.

- The development of a reconstruction approach that accounts for this knowledge during the inversion, that is a novel regularization approach.

1.6 Preliminary results

The preliminary results thus far are:

- A literature review of the optical properties to characterize the different tissue layers in the optical path of the adult human head; scalp, skull, meninges, gray and white matter.

- A first model of 4 layers with flat and homogeneous geometry based on the model of (Okada & Delpy, 2003) but extended for multiple wavelengths, as well as the inclusion of blood flow in the gray matter expressed as haemoglobin concentrations. Further, simpler models of 2 and 3 layers were built to set the decreased signal-to-noise ratio (SNR) with increasing tissue complexity.

- A colouration map (forward projection) was generated over two parameters, corresponding to discretized concentrations of oxy- and deoxyhaemoglobin for the visual cortex in a histologically plausible range.

- A first inversion (backward projection) based on the nearest-neighbour to outline the feasibility of a candid reconstruction without prior information.

These results and the way to achieve them are detailed in section 5. Although more detail is given later, as a summary, preliminary results show that with a 3 layers model (equivalent to some extent to the elimination of the contribution from the layer of the scalp), inversion is possible even in limited conditions, and the recovery of haemoglobin concentrations in cerebral cortex is viable. But this situation becomes unstable and the candid inversion is unable to recover haemoglobin concentrations in the gray matter when the tissue model is extended to include the scalp. These results are in agreement with the current concerns of the fNIRS community to avoid the influence of scalp introduced in the optical signal and we think this justifies the need to conduct this research. This results are still partial because blood flow has not been incorporated in the scalp layer, however, this inclusion shall just produce a noisier signal.

2 Theoretical Basis

2.1 Image formation and reconstruction

Image formation is the physical process by which light interacts with matter and the exiting radiation is sensed with a photosensitive device (camera, eye, etc) forming the scene. When a light source illuminates an object, the incident light might be reflected, absorbed and/or scattered (interaction) according to the optical properties of the object and spectra of the illuminant. The resulting exiting radiation, whether remitted or transmitted, abides to a certain spectral intensity distribution (SID). The image acquisition occurs when this SID is recorded by an optical sensor sensitive at that wavelength range.

Different models for image formation exists, like those shown in figure 1.
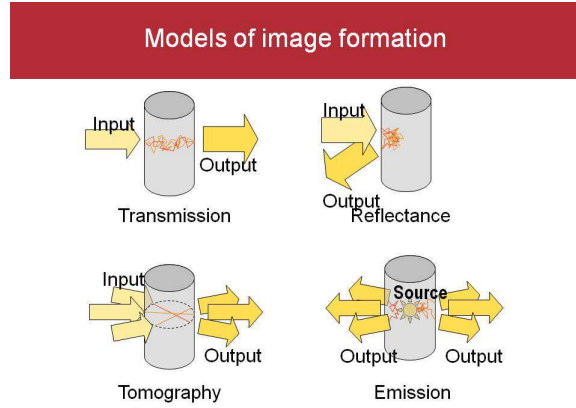
Figure 1: Different models of image formation.The reflectance model is used in optical neuroimaging for adult heads. Image borrowed from Prof. Claridge

Mathematically, the process may be modelled as a double mapping from the space of object's properties Π to the remitted (or transmitted) spectra first Λ , and from there to the image space I. Note the ambiguity in nomenclature of the last space, since the image of interest is the reconstructed one in the object properties space, and not the photometric captured directly by the image acquisition device.

$$G : \Pi \to \Lambda \quad F : \Lambda \to I \quad \Pi \in \mathbb{R}^n \quad I \in \mathbb{R}^m \tag{1}$$

Therefore, disregarding spatial aberrations, a pixel in the image observes:

$$i = F(G(\vec{\pi})) \tag{2}$$

The counterpart, image reconstruction is the process by which the properties of the object with which light interacted are recovered from the image observed radiation
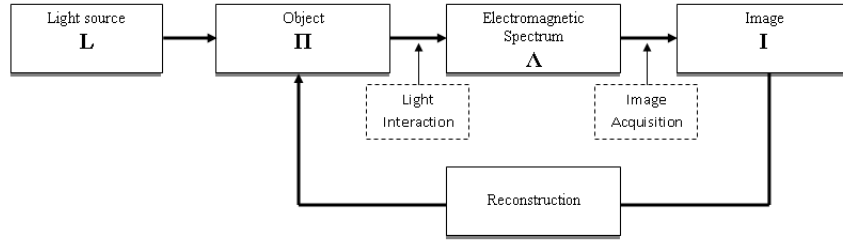
Figure 2: Image formation and reconstruction. When a light source L irradiates over an object Π light interaction produce a remitted electromagnetic spectrum Λ, this is acquired by a sensor to produce an image I. Reconstruction goes from the acquired image I to the object Π.

$F^{-1} : I \to \Pi$. Image reconstruction therefore refers to an inverse problem. Figure 2 illustrates both concepts.

2.2   Inverse problems

In a simple way, physical phenomena can be modelled mathematically as an associative relation like:

$$y = f(\vec{x})$$

Where, given a model f (forward model) and a vector of parameters $\vec{x}$ the effect y can be obtained.

Such problems arise under situations where it is not possible to measure directly the parameters of the system and need to be inferred from measurements in the boundary. This is the case in optical neuroimaging; this neuroimage, in the continuous wave modality, aims to retrieve the relative changes of haemoglobin oxygenated and reduced in the cerebral cortex in a differential way in time from measurements of diffuse reflectance in the scalp surface.

Inverse problems, often are ill-posed, i.e., they are not fulfilled with condition of well-posed problems defined by (Hadamard, 1902):

- The solution exists

- The solution is unique

- The solution's behaviour changes continuously with the initial conditions

In the inverse problem of optical neuroimage reconstruction, the first condition is fulfilled, since an observation y corresponds to a histophysiological truth, i.e., the

8

sensed light has been attenuated by the concentrations compounds in the tissue. The ill-posed problem is due to several reasons. First, the physics problem of image formation G is not monotonic throughout the whole in all the parameters' space, occurring that independently in different specifics wavelengths the chromophores separation be insufficient, effect known as *cross-talk*(Uludag *et al.*, 2002) so, this demands a suitable selection of wavelengths for a correct reconstruction. Second, due to the necesary discretization of the involved spaces in the image formation process, just a discrete representation is available of a continuous problem. Third, as during image acquisition -projection to a lower dimensionality- an undetermined system is obtained ($\Pi \in R^n, I \in R^m, n >> m$), violating the uniqueness criterion of the solution, causing that several parameters configurations $\vec{(\pi)}$ are reachable from the same observation $\vec{\lambda}$, effect know as *metamerism*(Preece & Claridge, 2004). Finally, the inherent noise in the measuring devices or the models approximating the physical phenomena (as well as other sources of noise) may alter the continuity of the solution. Therefore, small variations in sensed data may result in large biases in the solution. This problem of sensitivity of the data is inherent to the image reconstruction problem and not just of its computational approach. Commonly, to deal with ill-posed problems the inversion process requires a *regularization* method to avoid the problem of discontinuity in the solutions and ensure stability(Wang *et al.*, 2011).

2.3   Diffuse Optical Imaging

Diffuse optical imaging (DOI) is a promising imaging modality to study biological tissue non-invasively. It is based on the use of light to measure the optical properties of the tissue and create visual representations (Arridge & Schotland, 2009). This technique involves irradiating a light beam on the surface of the tissue to be imaged. Light propagates through the tissue where it suffers absorption and scattering by the various compounds forming the biological tissue. Part of the light that abandons the tissue, is captured by photoreceptors.

Particularly, in neuroimage, this technique is known as *functional Near Infrared Spectroscopy* (fNIRS) as it uses light in these wavelengths (600nm - 1000nm). In this optical window, light is able to penetrate the human head tissues deep enough to reach the cerebral cortex allowing interrogating the neural activity. The main characteristic that allows the use of this technique is because the physico-chemical processes produced in the tissue alter the light extinction as a function of the cellular metabolism. This makes possible the use of fNIRS for the detection of cortical haemoglobin concentration from measurements in the surface of the cerebral cortex. Figure 3 shows the operation of fNIRS.

Before light reaches the cortex it has to travel through several layers of tissue. Each of these layers is formed by different compounds and have a determined geometry that affects light propagation independently of the attenuation caused by the markers of neural activity to be measured. The figure 4 depicts an example of an image of the
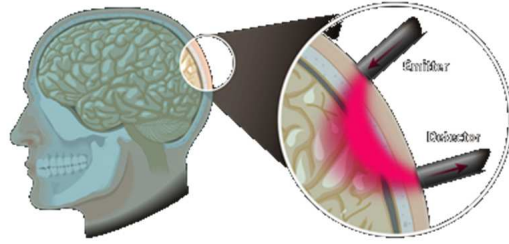
Figure 3: The operation of fNIRS is deceivingly simple. A light beam is irradiated into the tissue surface to be explored. Light propagates and part of it leaves the tissue and is captured by a photoreceptor. Figure reproduced from (resource:, 2015b)
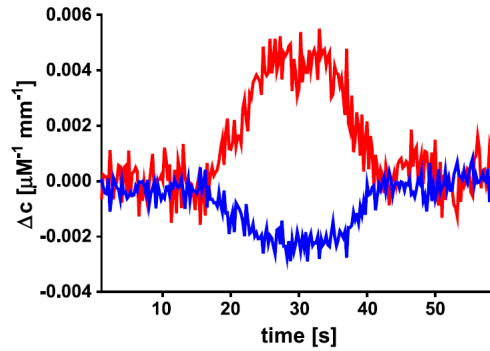
Figure 4: Changes in concentration of oxy (red) and deoxyhaemoglobin (blue). Figure reproduced from (Uludag *et al.*, 2004)

neural activity with fNIRS applying one the most common forward models(Modified Beer-Lambert Law -MBLL). The typical decrease of reduced haemoglobin concentration concomitant with increase HbO_2 concentration can be appreciated.

2.3.1   fNIRS modalities

The fNIRS signal can be measured in three different modalities (Strangman *et al.*, 2002) as shown in figure 5:

Continuous wave irradiates light at the tissue with constant intensity. Changes in light attenuation are interpreted as a consequence of brain activity. This modality is unable to distinguish light attenuation due to absorption and scattering. In contrast, it has the best signal to noise ratio. It is the most popular modality.

In the time domain modality, tissue is irradiated with a light pulse in the order of picoseconds and the photon's time of flight is measured. Time of flight is proportional to travelled path length, and thus photon coming from the cortex can be isolated by gating
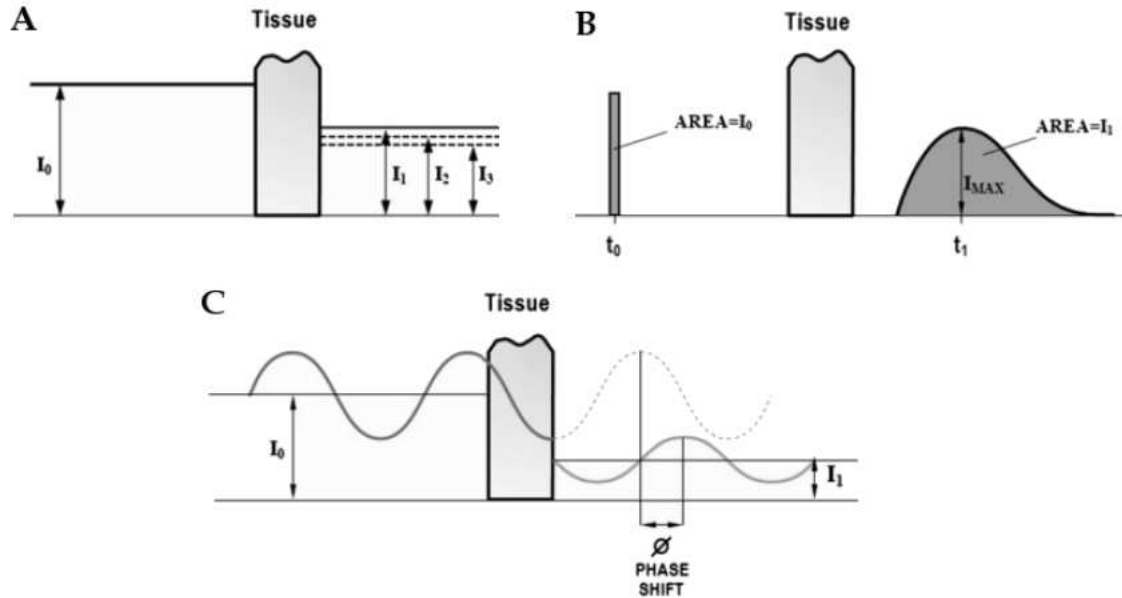
Figure 5: The three main measuring modalities in NIRS. a)Continuous Wave, b)Time Domain, c)Frequency Domain
. Figure reproduced from (Bakker *et al.*, 2012).

procedures. Its sensitivity is reduced because the little light intensity received.

Finally, the frequency domain uses light modulated in a given frequency. Changes in light attenuation and phase allow to estimate the optical properties of the tissue.

2.4 Anatomy and physiology of the human brain and head

The brain is protected by a set of tissues, namely: scalp, skull, meninges (Dura mater, arachnoid, pia mater) and cerebrospinal fluid (CSF)(Bear *et al.*, 2006) and its formed mainly by an outer layer named gray matter and an inner layer named white matter. It is estimated that in the gray matter reside over 100,000 million of neurons, while white matter is composed of the neuron's axons. Gray matter is where most of the brain activity occurs while the white matter is responsible of the communication between brain areas. Figure 6 shows a segment of the human head exhibiting the different layers.

The scalp is an important tissue in optical neuroimage becuase it absorbs much of the emitted light for spectroscopy (near to 76% (Haeussinger *et al.*, 2011)). It consists of five layers (Ellis & Mahadevan, 2013): Skin, Connective tissue, Aponeurosis, Loose connective tissue and Periosteum (Figure 7).The principal blood vessels of the scalp lie in the Connective tissue, and the scalp has the richest blood supply of any area of the skin. Moreover, the skin itself has an important blood supply in the dermis layer where there are blood vessels across the whole layer that act as absorbers of light(Claridge *et al.*,
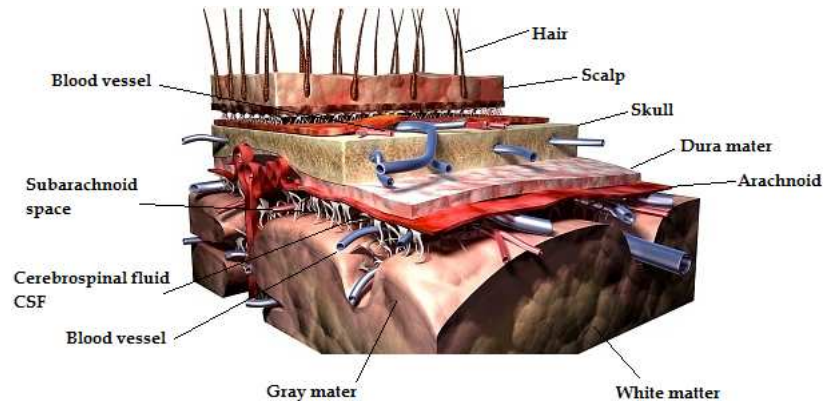
Figure 6: Representation of a segment of the human head where the layers that compose it can be appreciated. Figure reproduced from (resource:, 2015c).

2002).

2.4.1 Markers of neural activity

A number of physiological processes accompany brain activity. Those occurring at the level of a single neuron, and those occurring around its environment moderated by the neurovascular coupling (Villringer & Chance, 1997). The latter refers to those vascular events following neural activity. Such neural activity induces a vasodilation, consequence of the increment in oxygen consumption in the active region ($rCMRO_2$), permitting higher blood perfusion and increasing the flow ($rCBF$) and volume ($rCBV$) of blood to supply the active area with more oxygen. The increase in oxygen consumption following the neural activity induces, after a transient regional episode of blood deoxigenation, a massive response of blood irrigation increasing the oxygenated haemoglobin (HbO_2) and flushing out the reduced haemoglobin (HHb). Since the two species of haemoglobin have different absorption spectra it is possible to estimate their concentrations by means of spectroscopy. Figure 8 shows the absorption curves in the visible and infrared range of the spectrum of both haemoglobins as well as other molecules commonly present in biological tissues.

The direct electrical activity of the neurons is not observable with continuous wave fNIRS. The indirect observation of brain activity by means of diffuse optical imaging is possible because of the so called *neurovascular coupling*. This coupling is the phenomenon governing the brain haemodynamics as a response to oxygen consumption following neural firing. As afore mentioned, the alteration of the concentration of oxygen in blood is observable since the absorption signature of the oxygenated haemoglobin is distinct from that of the reduced species in the optical window. Figure 9 illustrates the neurovascular coupling.
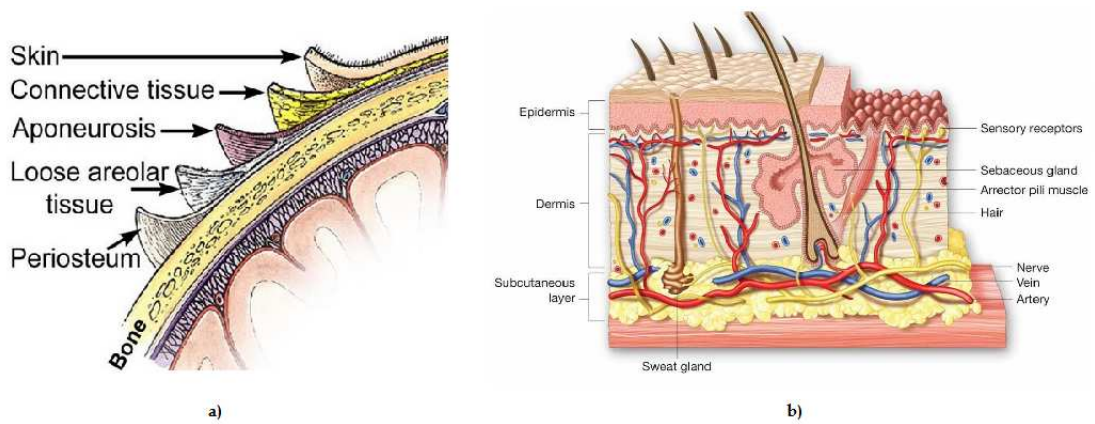
Figure 7: Main layers of the scalp a)and skin b). Figures reproduced from (resource:, 2015a).
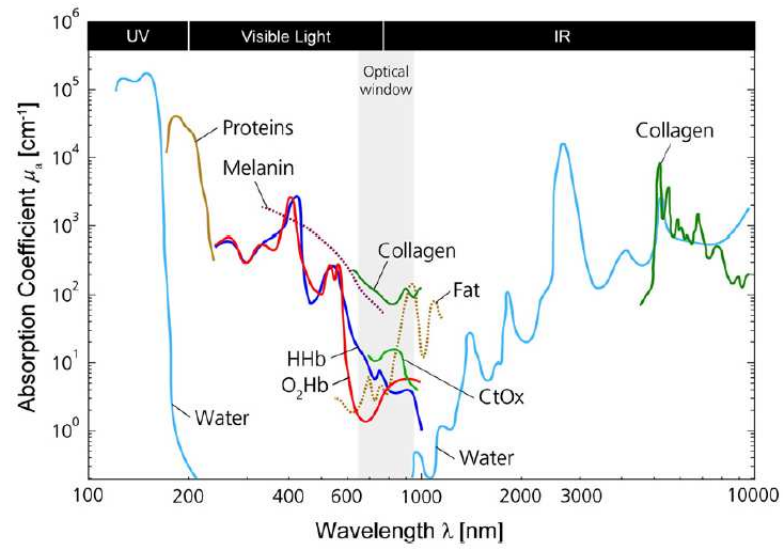
Figure 8: Absorption curves for both haemoglobin species and other tissue compounds in and around the near infrared range. Figure reproduced from (Scholkmann *et al.*, 2014).
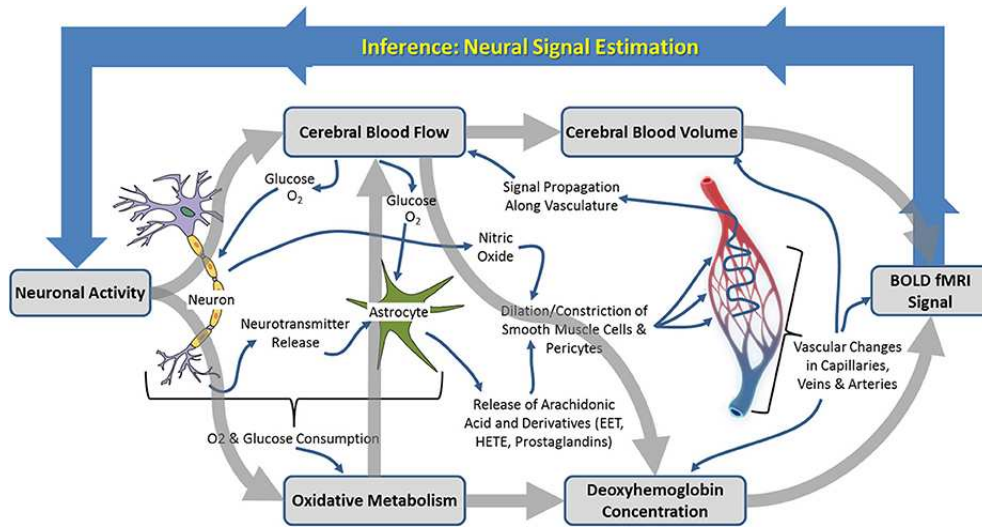
Figure 9: Schematic representation of the neurovascular coupling. Figure from (Martin, 2014). The illustration is prepared for the BOLD fMRI underlying neurovascular coupling is also exploited by fNIRS.

2.5 Radiation transport in matter

As electromagnetic radiation interacts with matter, several phenomena affect its propagation such as refraction, reflection, scattering and absorption. The former two occurs at the boundary of two different media, whereas the latter two occurs within a turbid medium. In general, these phenomena depend on matter, both its composition and its geometry, which are jointly referred to as optical properties.

Refraction is the change of propagation direction when light crosses from one medium to another. The refraction index n determines the speed of light within the medium as relative to the speed of light in vacuum (Branco, 2007) and refraction is governed by Snell's law (Orihuela-Espina, 2005).

Closely related is the phenomenon of reflection; when hitting the boundary between two media with different refraction index, part of the energy is bounced back or remitted at the surface of the new medium, an effect known as reflection. If reflected light rays are parallel and in a direction following the same but opposite angle to the incident ray, then it is referred to as specular reflection, and if such reflected light rays follow different directions then it is referred to as diffuse reflectance (Figure10).

Within the medium, as the light propagates, photons hit particles in the turbid medium suffering absorption events in which they transfer some of their energy to the particles, and such energy is transformed into another type of energy. This phenomenon is known as absorption and as a result of it the intensity of the travelling light becomes attenuated (Figure 1.a). The level of absorption in a biological tissue depends

14
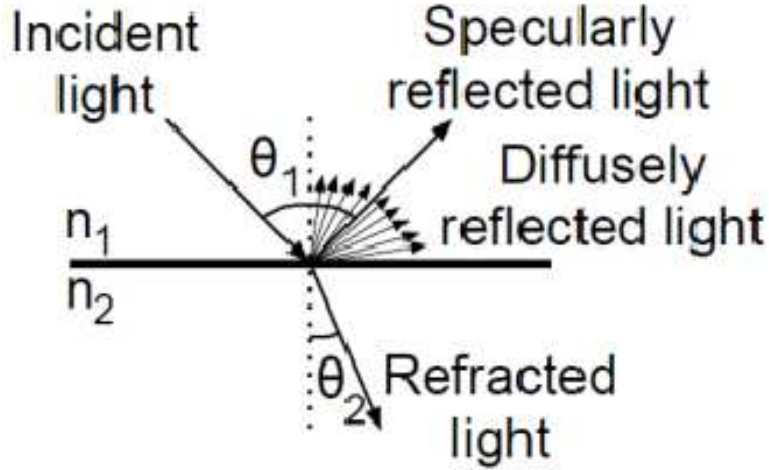
Figure 10: Schematic representation of light reflection and refraction. Figure reproduced from (Orihuela-Espina, 2005)

on its macroscopic absorption coefficient μ_a often expressed in mm^{-1}. This absorption coefficient represents the probability of a photon being absorbed by length unit.
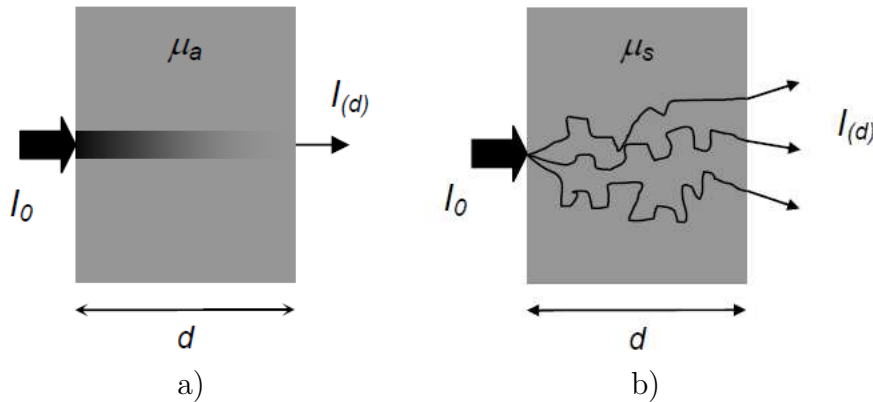
Table 1: Light attenuation due to absorption (a) and scattering (b) in a medium. Reproduced from (Branco, 2007)

Finally, scattering is the change of direction of a photon after the collision of the photon with a particle within the medium (Figure 1.b). Analogously, the level of scattering in a biological tissue depends on its macroscopic scattering coefficient μ_s often expressed in mm^{-1} which represents the probability of a photon being scattered by length unit.

Associated to tissue scattering is the property of isotropy or anisotropy. It refers

to the angular distribution of scattered light following a collision. Tissue an-/isotropy defines the likelihood that a given photon is dispersed in a certain angle Θ. When all directions are equally probable, then the medium is said to be isotropic, and otherwise is said to be anisotropic. Since biological tissue are mainly forward scatterers, this angular distribution is often only expressed over a single propagation plane; with the other angular distribution along the perpendicular plane -side scattering- being assumed as isotropic. Under this assumption, anisotropy may be expressed with a single anisotropy factor g representing the average value of the dispersion angle.

In the interactions events that photons undergo within the matter, some photon packages are fully absorbed whereas some other will retain some of their energy eventually becoming transmitted or backscattered to tissue surface. The former, referred to as transmittance, may be sensed with a transillumination setup but it is of little use in *in-vivo* non-invasive adult optical neuroimaging. Backscattered light arising at tissue surface is called remittance, and yet again if occurring in multiple directions it is referred to as diffuse and it is central to fNIRS.

The above phenomena are not fully described unless light wavelength (λ) of the propagating beam is taken into consideration, since the aforementioned properties are all dependent on the wavelength, i.e., the optical properties of the matter vary as a function of wavelength $n(\lambda), \mu_a(\lambda), \mu_s(\lambda), g(\lambda)$.

2.5.1 Models of Radiation Transport

Several methods have been developed to explain and estimate light propagation within matter. These models, capture with more or less detail, the radiation transport process and consequently allow to express the process of image formation. The following sections describe the radiation transport models frequently used in optical neuroimage.

2.5.2 Modified Beer-Lambert Law

The Beer-Lambert Law (BLL) is a model that describes the loss of light intensity (I) due mainly to absorption as a function of the concentration of a substance in a non-scattering medium (equation 3).

$$I = I_0 \exp^{-\epsilon(\lambda)cd} \tag{3}$$

Where I_0 is the incident light, ϵ is the specific extinction coefficient of the medium (wavelength dependent), c is the concentration of the cromophore[1] responsible for the extinction and d the thickness of the medium.

Since biological tissue is highly scattering and in order to use the relation defined by this law, an extension known as the Modified Beer-Lambert Law (MBLL), was developed by (Delpy *et al.*, 1988). This extension incorporates two elements to the BLL:

---

[1]A chromophore is the part of a molecule responsible for its color. The color arises when a molecule absorbs certain wavelengths of light and transmits or reflects others.

the Differential Path-length Factor (DPF) that accounts for the increased distance that the light travels due to scattering, from light source to detector, and a factor G accounting for tissue geometry and light attenuation due to scattering (Boas *et al.*, 2011; Scholkmann *et al.*, 2014). So the MBLL is expresed as:

$$I = I_0 \exp^{-\epsilon(\lambda)*c*d*DPF(\lambda)+G(\lambda)} \tag{4}$$

A more general representation of the MBLL is show in equation 5 that express the loss of light intensity (Optical Density - OD or Attenuation, unitless) in time and as a linear combination of all present chromophores.

$$OD(t, \lambda) = -\log_{10}\left(\frac{I(t, \lambda)}{I_0(t_\lambda)}\right) = \sum_i \epsilon_i(\lambda) * c_i * d * DPF(\lambda) + G(\lambda) \tag{5}$$

This law is used in optical imaging under the assumption that the change in scattering is small compared to changes in absorption in time. So, factor $G(\lambda)$ is assumed to be time-invariant. In this way, determining changes in OD in two consecutive measures, t_0 and t_1, the term $G(\lambda)$ can be neglected and relative changes ΔOD can be estimated by the difference:

$$\Delta OD(\Delta t, \lambda) = OD(t_1, \lambda) - OD(t_0, \lambda)$$

$$\Delta OD(\Delta t, \lambda) = -\log_{10}(\frac{I(t, \lambda)}{I_0(t_\lambda)}) = \sum_i \epsilon_i(\lambda) * \Delta c_i * d * DPF(\lambda)$$

Where the chromophore concentration $\Delta c_i = c_i(t_1) - c_i(t_0)$ is a relative change in concentration in time.

The MBLL is the most common forward model currently used in fNIRS (Scholkmann *et al.*, 2014). Nevertheless, because of the strong assumptions on scattering and geometry, the MBLL does not hold true for measurements of the head (Boas *et al.*, 2011). Moreover, the strongest assumption with the MBLL to be used for neuroimage is that the changes in attenuation are all attributable to changes in haemoglobin occurring directly in the cerebral cortex.

2.5.3   Radiative Transfer Equation

The more general model of light propagation is the Radiative Transport Equation (RTE) or Boltzmann equation (Eq. 6)(Branco, 2007)

$$\frac{1}{c}\frac{\partial I}{\partial t} + \nabla I(r, t, \hat{s}) + (\mu_a + \mu_s)I(r, t, \hat{s}) = \mu_s \int f(\hat{s}, \acute{\hat{s}})I(r, t, \hat{s})d^2\hat{s} + q(r, t, \hat{s}) \tag{6}$$

Where $I(r, t, \hat{s})$ is the radiance at point r, in time t and direction $\hat{s}$, c is the speed of
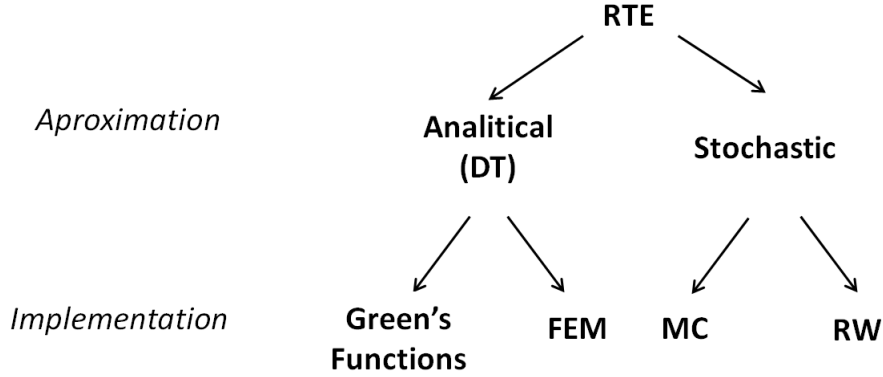
Figure 11: Scheme of the different models derived for the RTE commonly used for optical imaging and its respective implementations.

light in the medium, μ_a and μ_s are the absorption and scattering coefficients respectively, $f(\hat{s}, \acute{\hat{s}})$ is the scattering phase function which define the scattering change direction (from $\hat{s}$ into $\acute{\hat{s}}$). Finally, the term $q(r, t, \hat{s})$ is the light source.

The RTE follows from the Maxwell equations when the latter are applied to the problem of multiple electromagnetic scattering in discrete random media (Mishchenko, 2003). This is an energy balance equation that has into consideration the changes in energy flow, in time and in an infinitesimal volume, due to gain of incoming energy by a light source or by scattered photons and energy lost due to photons leaving the volume and absorbed energy.

Exact solutions to the RTE are limited in practice to simple cases where the propagation medium has simple geometry and isotropic scattering (Branco, 2007). Given these restrictions, other models have been derived that approximate the RTE (Dehghani *et al.*, 2009b) (see Figure 11) in order to be useful in practical applications. For each approximation, there are different implementations which are summarized in Figure 12. This figure summarizes the implementation of the main approaches used in optical image and some of their advantages and disadvantages.

Figure 12 indicates that FEM methods are computationally fast. This is true in this domain by two reasons: first, the structure of the mesh used is not too complex and second, the consuming time of mesh generation is not considered which is known to consume 70% of the computation time (Muñoz-Gómez *et al.*, 2005). However, actually there exist methods to avoid the mesh generation, such as: meshless methods (Kansa, 1990) which use random set of nodes in which the solution is computed. A method to solve Partial Differential Equations explored recently are the so called Smooth Particle Hydrodynamic. However, these methods are out of the scope of this work.

Monte Carlo methods involve simulating the interaction of single photons within the matter through the use of probabilities that define photons events. In order to achieve

Aproximation	Implementation	Advantage	Disadvantage
Diffusion Theory	Green's Functions	Fast computationally	Simple geometries
	Finite Element Method	Complex geometries Inhomogeneous media	No means of deriving individual photon histories Need special methods to deal with void regions
Stochastics	Monte Carlo	Computational speed Simple implementation Complex geometries Inhomogeneous media Naturally deal with void regions Able to trace photon paths	High computational cost Accuracy proportional to number of photons Strong dependency of optical properties
	Random Walk Theory	Simple implementation	Restricts photon's scattering directions

Figure 12: Summary of advantages and disadvantage of some models that approximate the RTE.

useful estimations millions of photons have to be simulated. In consequence, this method is computationally expensive.

2.6 Image reconstruction

The image reconstruction process aims to recover the internal properties of the tissue from the measurements recorded. This involves the solution of the forward and inverse problems (Arridge, 2011; Branco, 2007).

The forward problem (Eq. 7) relates to predict the measurement y, through the use of a photon propagation model F, from a given set of optical properties π in order to approximate as close as possible the measurements in the real world.

$$y = F(\pi) \tag{7}$$

The complementary inverse problem relates to the recovery of the hidden parameters π from the measurements y; $\pi = F^{-1}(y)$. Several authors (Dehghani *et al.*, 2009b; Arridge & Schotland, 2009; Branco, 2007), classify methods in image reconstruction as linear versus non-linear.

2.6.1 Linear methods

Linear methods are the simplest way to address the reconstruction problem. These methods are able to obtain images of temporal changes in optical properties (Dehghani *et al.*, 2009a) and require a difference experiment that measure $\Delta y = (y_1 - y_0)$ as the difference of optical changes $\Delta \pi = (\pi_1 - \pi_0)$.

2.6.1.1 Perturbation method

Perhaps the simplest of them all is the so called perturbation method. Given an estimate $\hat{\pi}$ close to the solution π, then assuming continuity an estimate $\hat{y} = F(\hat{\pi})$, with the

19

forward model is close to a real measurement y. By expanding Eq. 7 with Taylor series:

$$y = F(\hat{\pi}) + F'(\pi)(\pi - \hat{\pi}) + (\pi - \hat{\pi})^T F''(\pi)(\pi - \hat{\pi}) + \cdots \tag{8}$$

Where F' and F'' are the first and second derivatives of the forward model. Neglecting second and higher order terms, the linear term constitutes the *perturbation approach* (Arridge & Hebden, 1997). In discrete cases the derivative F' can be expressed as a matrix J, known as the Jacobian (or sensitivity matrix). Now, considering $\Delta y = (y - \hat{y})$ and $\Delta \pi = (\pi - \hat{\pi})$, the linear equations system to solve is (Eq.9):

$$\Delta y = J(\hat{\pi})\Delta \pi \tag{9}$$

The reconstruction problems reduces to solving the linear system in Eq. 10 by inverting the Jacobian Matrix J.

$$\Delta \pi = J^{-1}(\hat{\pi})\Delta y \tag{10}$$

2.6.1.2 Reconstruction with MBLL

The MBLL described in section 2.5.2, can be used to recover the information of interest in fNIRS. The reconstruction method is the system of equations derived from the MBLL itself. We need measurements in time t_0 and t_1 in order to get the $\Delta OD(\Delta t, \lambda)$ in equation 5. Finally, to obtain the concentration changes of the n chromophores of interest, that equation should be evaluated at n different wavelengths. Then, the resulting system to solve is:

$$[\Delta C_i] = d^{-1}[\epsilon_i(\lambda_j)]^{-1}[\Delta OD(\Delta t, \lambda_j)/DPF(\lambda_j)] \tag{11}$$

2.6.2 Non-Linear Methods

Non-linear reconstruction are iterative methods based in optimization looking for minimizing the difference between the values calculated by the forward model and the experimental data while the sensitivity matrix J is updated in each iteration (Jiang *et al.*, 1996).

There are two main approaches for such optimization (Dehghani *et al.*, 2009a): gradient-based reconstruction (Zhu *et al.*, 1997; Arridge & Schweiger, 1998) and Newton-like methods. The latter requires the calculation of the Jacobian and its inversion. In general, the procedure followed in this methods is depicted in figure 13 and proceed as follows: given an initial guess of the optical parameter under study (μ_0), a measure $\hat{y} = G(\mu_0)$ is computed with the forward model given the initial parameter. From these, the Jacobian matrix is calculated (J). The distance between $\hat{y}$ and an experimental data y is measured. If the distance is greater than a given threshold the

Jacobian have to be inverted and regularized in order to estimate a new value for μ. The method iterates until the parameter μ has been closely approximated.

2.6.3 Alternative approaches

In the following sections we describe other approaches that have been used to solve the inverse problem of image reconstruction. Their advantage is that the inverse problem is solved implicitly without need to calculate the Jacobian. The prize to pay is often explanatory power.

2.6.3.1 Colouration map

The Colouration Map has been used in works of Claridge *et al.* (2002); Orihuela-Espina (2005); Claridge & Hidović-Rowe (2014). In this method, the space of parameters to be recovered is discretized and each vector is projected to the spectral space through the forward model. Each remitted spectra is convolved with a response function simulating image acquisition process by a device and projecting each spectrum to the image space. The image space (Colouration Map) becomes a look up table in which new observations can be approximated looking for the estimated parameter $\hat{\pi}$ such that:

$$\hat{\pi} = \underset{\vec{\pi}}{\operatorname{argmin}} \, ||F(\vec{\pi}) - \vec{i}|| \tag{12}$$

In Claridge & Hidović-Rowe (2014) model inversion is implemented using a Discrete Markov Random Field (DMRF) optimization using an Iterated Conditional Models algorithm which maximize the probability of each variable in the DMRF to get the parameter $\vec{\pi}$ with highest probability. An important aspect to consider in this method is the discretization of the parameters space, which has a direct effect over the inversion (Orihuela-Espina, 2005).

2.6.3.2 Machine learning

Because of the increasing popularity of machine learning algorithms, these methods have been applied in some inverse problems. However, we are unaware of any application related to neuroimage reconstruction.

These methods require samples from which the algorithm can be trained, of the form $(\vec{\pi}, y)$, being $\vec{\pi}$ the parameters to reconstruct and y the associated observation. Although, they are able to achieve high scores in classifying a given observation (and recovering parameter $\vec{\pi}$) generally they are not useful in the field of neuroimage because the lack of explicative capacity needed to understand what is going on inside the tissue. Neverless, a lot of the useful applications of machine learning algorithms in brain imaging is characterizing states of the brain through the imaged signal for tasks, as for example, in Brain-Computer-Interface(BCI)(Lemma *et al.*, 2011).
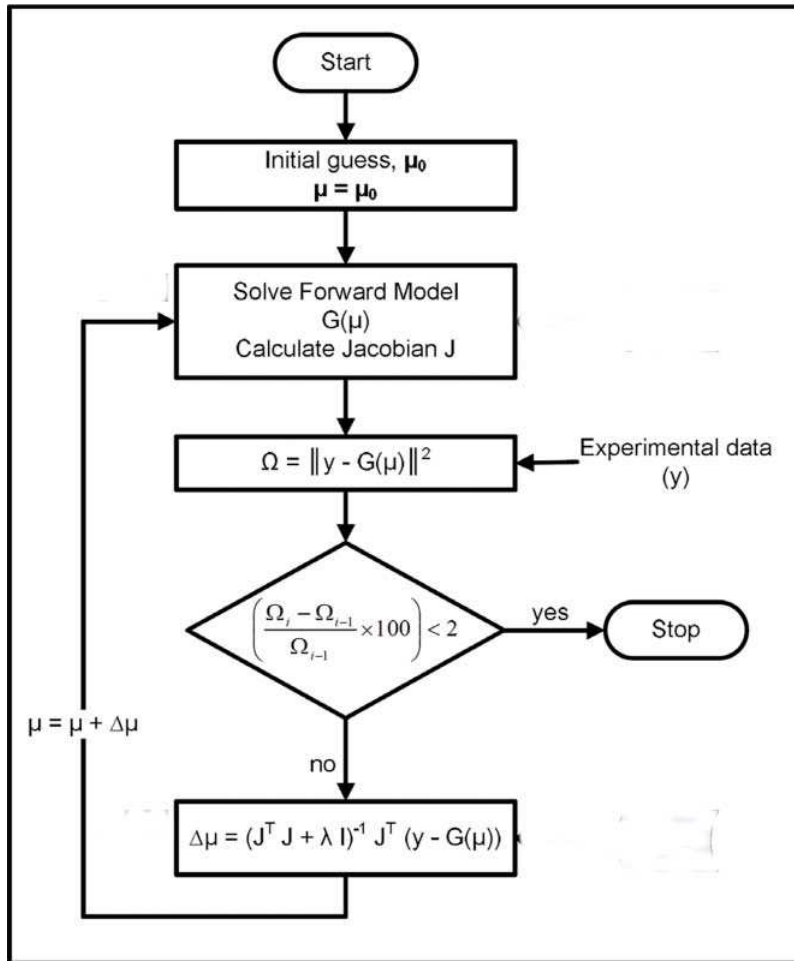
Figure 13: The flowchart shows the main steps in the iterative methods for reconstructing optical parameters in diffuse optical imaging. Figure reproduced from (Prakash *et al.*, 2010).

3 Related Work

3.1 Monte Carlo forward models of the adult head

Several authors have developed forward models of the adult head using the Monte Carlo approach as light propagation method. These models have served for the study of many phenomenons in optical imaging and more specifically in fNIRS. Many of these models are far from a realistic anatomy of the brain both in geometry and histology. Some use flat layers of the tissue (simple square geometry) and others use structural images from magnetic resonance (MRI) segmenting each layer manually or semi automatically. Further, many of these models assume an homogeneous structure of the layers, i.e., the optical properties are constant within each layer.

The characteristics of some of these models are summarized in table 2.

Work	Intention	Model			
		Geometry	Homogeneous/ Inhomogeneous	# layers	Layers
Guo2013	Wavelength selection and Source-Detector spacing analysis	Flat	Inhomogeneous	4	Scalp-Skull,CSF,Gray and White matter
Bocklin2012	Determining 3D light distribution in human head	Based on MRI	Homogeneous	5	Scalp,Skull,CSF,Gray and White matter
Takahashi 2011	Influence of skin blood flow on near-infrared spectroscopy	Flat	Homogeneous	5	Scalp,Skull,CSF,Gray and White matter
Custo2006	Effective scattering coefficient of the cerebral spinal fluid	Based on MRI	Homogeneous	5	Scalp,Skull,CSF,Gray and White matter
Kim2005	Effect of the refractive index in the CSF	Flat	Homogeneous	5	Scalp,Skull,CSF,Gray and White matter
Uludag2004	Wavelength selection	Flat	Homogeneous	10	Synthetic layers
Franceschini2004	Study of the Fast-optical-signal	Based on MRI	Homogeneous	5	Scalp,Skull,CSF,Gray and White matter
Okada2003	Scattering effect of the CSF and the arachnoid	Flat	Homogeneous	6	Scalp,Skull,CSF,Arachnoid, Gray and White matter
KohlBareis2002	Separation of brain from skin and skull signals	Flat	Homogeneous	10	Synthetic layers

Table 2: Head models proposed by several authors relying on Monte Carlo approach for radiation transport.

3.2 Current solutions to capture blood irrigation to scalp

Several works have intended to de-noise the fNIRS signal from the skin blood flow noise through the use of signal processing approaches, like wavelets, Multi-Resolution Analysis or statistical approaches (Tachtsidis *et al.*, 2010; Scholkmann *et al.*, 2014). For this purpose, the systemic effect altering the fNIRS signal is measured with specialized devices.

In the case of the blood flow in the scalp a Laser Doppler has been used (Patel *et al.*, 2011). Other approaches try to avoid its effect detecting the signal in the scalp with optodes in the NIRS device and resting its contribution for the signal (Takahashi *et al.*, 2011) thus complicating the hardware. Table 3 shows some of the works and the approaches to eliminate the blood irrigation in the scalp.

Work	Intention	Measuring blood flow [Concurrent measurement/ Transient / Multiple Channels	Methods for de-noising
Kirilina 2013	Quantifying physiological noise in fNIRS and denoise signal	Concurrent measurement	Wavelet Coherence Analysis General Linear Model
Tanaka 2013	Extract task-related components to fNIRS	Transient	Task-related component analysis
Funan 2013	To quantify the effect of absorption changes in scalp	Multiple Channels	Independent Component Analysis
Zhang 2012	Suppress physiological interference	Multiple Channels	Recursive least-squares (RLS) algorithm
Patel 2011	Quantification of systemic Interference	Concurrent measurement	Independent Component Analysis
Takahashi 2011	Influence of skin blood flow on near-infrared spectroscopy	Multiple Channels	Signal substractions
Tachtsidis 2010	Analisys of the fNIRS signal with and without systemics changes	Concurrent measurement	General Linear Model
Kohno 2007	Removal of the skin blood flow	Transient	Independent Component Analysis

Table 3: Approaches to account for the effect of the blood flow in the scalp.

3.3   Image reconstruction for diffuse optical imaging

As described in section 2.6 the goal of image reconstruction is the recovery of parameters. The table 4 summarizes some of the relevant reconstruction approaches related to optical imaging.

Several authors have given insights about how prior knowledge, such as the anatomical geometry of the head, physiological information, spatial or spectral relations can be incorporated into the inverse problem to improve reconstructing(Baillet & Garnero, 1997; Dehghani *et al.*, 2009a; Okada, 2013; Claridge & Hidović-Rowe, 2014).

Work	Tissue	Forward problem	Reconstruction	a prior	Evaluated
Prakash 2014	Breast	Diffusion Theory	Newton-like optimization	None	Synthetic data Phantom
Claridge2014	Colon	Monte Carlo	Colouration Map Markov Random Filed	Spatial regularization	Synthectic data Histologycal analysis
Dehghani2009	Breast	Difussion Theory - FEM	Newton-like optimization	Spectral (wavelengths) Spatial (regions)	Synthetic data Phantom
Dehghani2009b	Brain	Difussion Theory - FEM	Newton-like optimization	None	Synthetic data
Jiang 2000	Unknown	Difussion Theory - FEM	Newton-like optimization	None	Synthetic data
Maki 1995	Brain	MBLL	Ax=b	None	Real data

Table 4: Related works in image reconstruction.

4 Research proposal

4.1 Problem Statement

A lot of the research in the field of diffuse optical image concentrates on finding solutions to remove artefacts, whether inherent to physics of radiation transport, or consequence of a naturally imperfect sensing device (Orihuela-Espina *et al.*, 2010). Eliminating undesired contributions to the signal permits establishing an inverse projection from the sensed information closer to the physiological true.

Being ill-posed, the reconstruction problem demands the imposition of constraints to guarantee uniqueness of the solution. These constraints take the form of specific assumptions about the acquisition unit or more commonly in the form of simplifications regarding the tissue composition, optical properties or geometry.

The problem that we address in this research is on the one hand, the quantification and better understanding of the effect of haemoglobin concentration in the scalp, and on the other hand, the development of a computational reconstruction solution that retrieves the information of interest, proxy of the neural activity, in a cleaner manner reducing the noise from the systemic effect of scalp irrigation.

From a more general point of view, the challenge involves establishing a map between two spaces given certain constraints. To illustrate this conceptualization of the problem, let's take as an example the continuous bidimensional space Π in the left of Figure 14. Every point in Π represents a vector of parameters corresponding to a certain set of histophysiological compounds of interest with specific values $\vec{\pi} = (\pi_1, \pi_2)$. Through the image formation process (represented by function F), each parameter vector is projected into space I (center panel of Figure 14). In this synthetic example the projection function has been (manually) defined following an explicit analytical form for F -as indicated in the Figure-, and it would suffice to find F^{-1} to be able to retrieve the original vector $\vec{\pi}$ in Π associated to any observed vector $\vec{i}$. However, in a real scenario, several sources of noise affect the projection of every point, resulting in a space such as the depicted in the right panel of Figure 14. Consequently, reconstruction becomes aggravated.
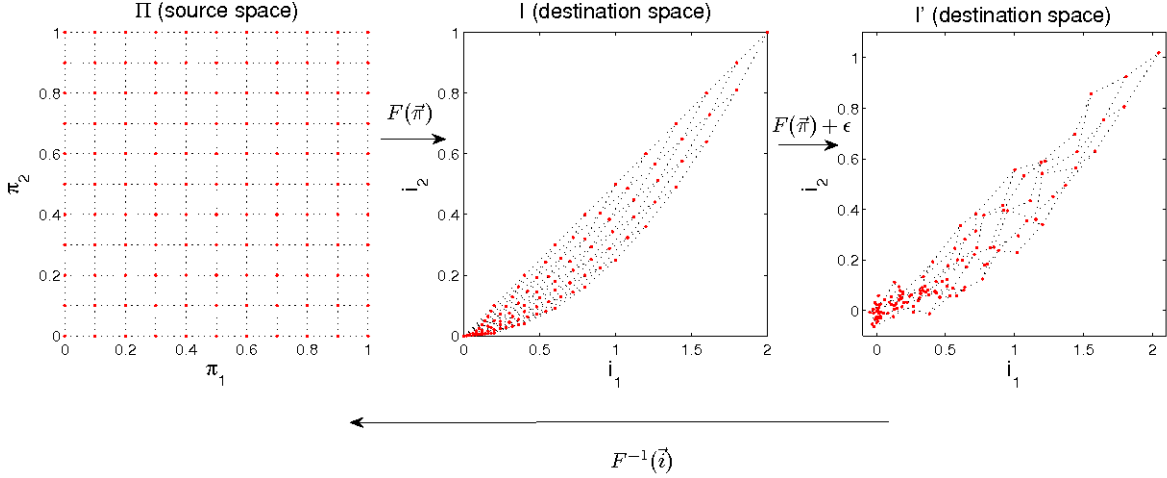
Figure 14: The figure illustrates a a fictitious non linear mapping from parameter space Π to image space I and noisy space I'. In this particular example the mapping is manually defined as $F(i_1, \imath_2) = (2\pi_1\pi_2, \pi_1\pi_2^2)$. Intuitively, points in the most bended region of I space (around the origin in this example) will have very low tolerance to noise. The reconstruction involves recovery of originating locations in space Π from observations in space I' without explicit knowledge of mapping F. In the case of diffuse optical imaging, knowledge of physics allow us to express $\bar{F} \approx F$

However, in the real scenario, the explicit analytical form of F is not available, That is, the forward model F can't be expressed as a combination of functions known until now. Under these circumstances, the inversion problem becomes that of estimating an approximation to F^{-1}; this problem may be expressed in a generic case as follows (Claridge & Hidović-Rowe, 2014): for every observed intensity vector $\vec{i}$, find a vector of parameters $\hat{\pi}$ such that:

$$\hat{\pi} = \underset{\vec{\pi}}{\operatorname{argmin}} ||F(\vec{\pi}) - \vec{i}|| \tag{13}$$

In addition, in the image formation process several other ingredients are involved affecting the recorded signal; from biological compounds naturally present in the tissue but that are not of interest for decoding brain activity in this case, to external factors such as uncertainty in the photodetectors response, or the environmental conditions among others (Orihuela-Espina *et al.*, 2010). Hence, in the inverse problem of image reconstruction the observations are contaminated with noise that significantly distort the estimations and thus violating the third postulate of Hadamard. It is in this state of affairs that an adequate inversion model and the implementation of a regularization approach are indispensable, and this research advocates for a solution that considers *a priori* information of the domain. This *a priori* information will reduce the search space

26

by fixing some of the parameters involved in the image formation process allowing the reconstruction process to consider information just in the space of interest.

The computational problems addressed in this research are summarized in Table 5.

Problem	Computational problem	Proposal
Image formation	Modelling of the forward problem $y = F(\vec{\pi})$	Forward model expressing realistic head anatomy and blood flow in gray matter and scalp
Quantify the effect of blood in scalp	Evaluation of error (SNR)	Optical characterization of its effect
Image reconstruction	Regularization methods	Include *a priori* information to improve stability

Table 5: Summary of problems and proposal to each one that contribute in the state of the art

4.2 Research questions

The following questions will guide this doctoral research in order to achieve the scientific contributions in the thesis topic.

Q1 Is attenuation of the effect of skin blood flow possible by means of informing the inverse process with prior knowledge of its quantitative contribution to the remitted spectra leaving a clearer reconstruction of the brain haemodynamics?

This is the central question to this thesis; as far as the author is aware this issue of scalp noise has not yet been addressed by means of enhancing the inversion strategy. Answering this requires (i) an accurate forward model permitting estimation of scalp irrigation to remitted spectra, and (ii) a new way to express physiological constraints in the inversion, none of which appear to be currently available in literature.

Q2 Does systemic and/or task evoked changes in scalp irrigation leave a traceable (quantifiable) and predictable (monotonic under certain constraints) imprint in the remitted spectra from the adult head?

In absence of scattering and with a single absorber, the Beer-Lambert law prescribes that higher concentrations in a chromophore will increase attenuation and

consequently its concentration is quantifiable from optical density measurements. However, as tissue becomes more complex, the monotonic recipe of Beer-Lambert no longer can be guaranteed which is especially true if more than one chromophore is concurrently altering its concentration. This question aims to elucidate the effect of blood flow to scalp over the remitted spectra.

Q3 If the effect of blood flow to scalp over the remitted spectra, can uniqueness of solution to the reconstruction problem be guaranteed throughout the entire physiologically plausible range?

Even if contribution to remitted spectra from known physiological vectors is measurable (positive answer to Q1), and even if this predicted attenuation can be exploited to enhance reconstruction under specific circumstances i.e. specific locations of the parameters' space (positive answer to Q2), uniqueness throughout the whole region of physiologically plausible range has to be demonstrated giving validity to the model

4.3 Hypothesis

Following the research questions it is hypothesized that:

The reconstruction of the haemodynamics markers (relative concentrations of haemoglobin) of neural activity in optical imaging can be achieved more precisely once the effect of the haemoglobin in the scalp has been avoided.

Here **more precise** means giving an approximation closer to the true solution.

4.4 Aim

To develop and validate a computational solution to circumvent the degeneracies introduced by systemic scalp blood flow in the reconstruction of markers of brain activity , and thus permitting a cleaner reconstruction of the optical neuroimage.

4.5 Key objectives

O1. Optical characterization of different parameters of the tissue and their contribution to the remitted spectrum given the defined forward model.

O2 Definition and development of a forward model of the adult human head considering realistic geometry and the haemodynamic in the gray matter and the blood irrigation in the scalp.

O3 To develop a computational solution to the image reconstruction problem to obtain the neural activity in a more clearly way considering knowledge of the noise produced by the blood irrigation in the scalp.

O4 To internally validate the solution to ensure an stable behaviour.

4.6 Contributions

- A better understanding of the diffuse optical neuroimage formation process through the assessment of the contribution to the final remitted spectra of a set of histo-physiological parameters.

- The specific quantification of the attenuation introduced by blood irrigation to the scalp within histologically plausible ranges.

- The development of a reconstruction approach that accounts for this knowledge during the inversion.

An indirect contribution of this work will be the way in which the *a priori* information will be incorporated into the regularization problem. This could be extrapolated to other domains where regularization is needed and *a priori* information is available in order to obtain a numerically stable solution.

4.7 Methodology

Figure 15 shows the elements involved in the process of image formation in the real world and the corresponding process in a computational model, from the image formation, acquisition and reconstruction of the parameters of interest.

The following methodology is proposed to reach every objective in this research

- Optical characterization of the tissues of adult human head. Initially, a set of major tissues (scalp, skull, meninges, gray matter, white matter) and compounds (Hb in cortex and scalp) will be considered. Experimental estimation of optical properties of these elements is not part of this thesis; this work will rely on values published in literature. However, it is likely that the extinction coefficients of all elements of interest may not be available at some or all the infrared region. In this case approximation e.g. by interpolation, substitution for animal model values, or reasonable assumptions shall be made prioritizing that order.

- To approximate the forward model to a more realistic anatomy of the human head, either structural images of magnetic resonance or CT from the head will be used. In the case of opting for the first alternative, 3D segmentation of tissues of interest whether automatic, semi-automatic or manual will be needed.

- With the Monte Carlo approach, as radiation transport model, and the human head model defined previously, the forward model will be determined over which the effect of the haemoglobin can be studied. The forward model will be validated in order to confirm its ability to generate spectra that could be fitted. Several

simulations will be performed varying their histophysiological ranges to evaluate the contribution of every tissue and compound in the remitted spectrum. This will reveal the sensitivity of each layer in our model and their possible contribution during inversion.

- Refining the forward model. Later, a more detailed second model will be defined. This will for example, model the skin in the scalp (dermis, epidermis, subdermis) and meninges in more detail. Again, optical characterization will follow similar process that in the first step.

- Quantification on the diffuse reflectance of the effects of the concentrations of oxygenated haemoglobin and reduced in 4 variables model parameters: HbO2 and HHb in the scalp, HbO2 and HHb in the cerebral cortex . These will be considered to influence both absorption and scattering (under single scattering regime). Histologically plausible ranges will be obtained from literature for several regions of the brain, and under different circumstances for the scalp e.g. systemic or task-evoked.

- A colouration map will be generated for the haemoglobin variations considering the wavelengths that best separate each chromophore according to literature. The problem of wavelength selection for reduction of cross-talk at acquisition time is not considered here. If necessary, image acquisition might be simulated by filtering remitted spectra with assumed optical efficiency of the photodetector.

- Preliminar reconstruction. An initial reconstruction approach based on the nearest neighbour over the colouration map will be implemented to establish distinction capability . To evaluate the reconstruction, synthetic data will be generated with the forward model altering the concentration of the haemoglobin considering all possible cases: increase/decrease Hb in gray matter with/without Hb in the scalp in all the plausible ranges.

- Another approach for reconstruction based on the perturbation method will be developed to improve the parameters recovery and evaluate the advantage of this method.

- Incorporation of priors to inversion. As was mentioned in section 3, is possible include *a priori* information to deal with ill-posed problems and hence improve reconstruction. The information about the effect of the blood in the scalp will be incorporated to the regularization process. The needed regularization parameter λ will be calculated by optimization methods.

- Once the model and the reconstruction approach have been accomplished and extensively tested with synthetic examples, the reconstruction will be validated with an optical phantom and/or real data depending on time availability. Real data if necessary are expected to be obtained from a device currently being developed at

Measurement	oxy, deoxy and total haemoglobin concentration
Light source	Laser diodes 650nm and 830 nm
Channels	24
Emitters	10
Detectors	8

Table 6: Summary of characteristics of a fNIRS device

our institution, but acquisition at external institutions may be considered. Internal and apparent validity will be performed.

Following, the characteristics of a commercial NIRS device are summarized in Table 6.
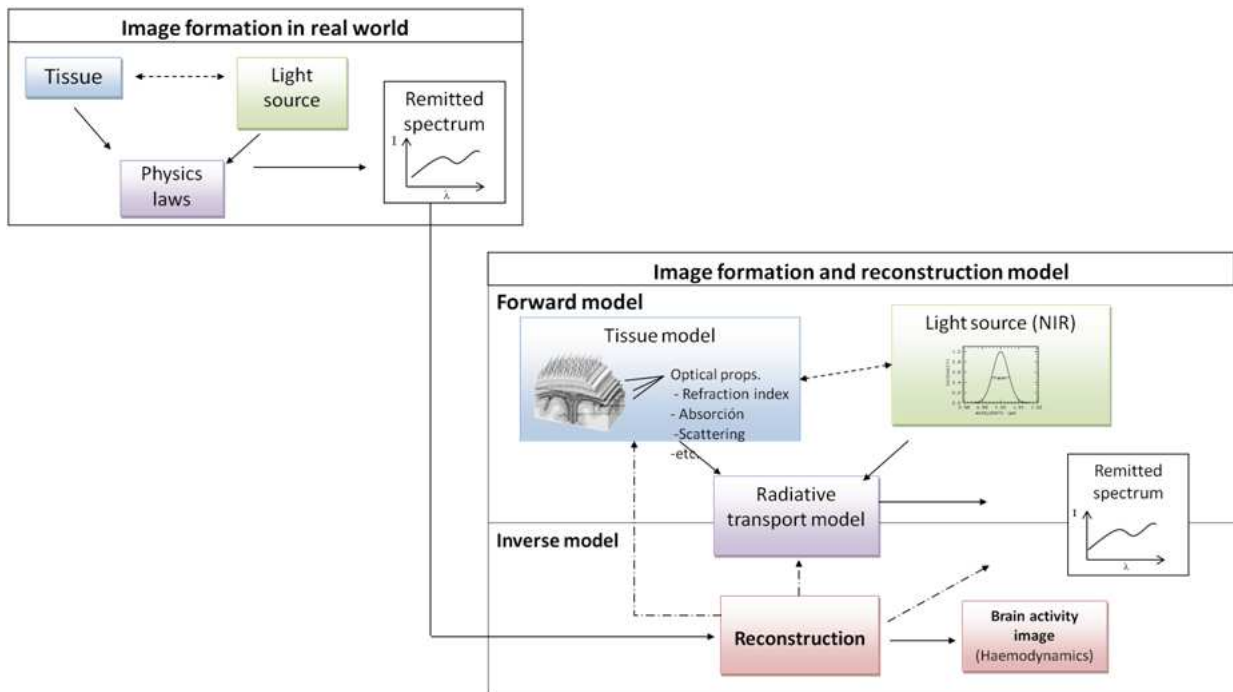

Figure 15: Schematic representation of the whole process, both in real world and the computational model.

4.8 Plan

The schedule in Figure 16 of activities for the realization of this research is proposed.

| | 2014 | | | | | | | | | | | | 2015 | | | | | | | | | | | | 2016 | | | | | | | | | | | | 2017 | | | | | | | | | | | |
Activity	1	2	3	4	5	6	7	8	9	10	11	##	1	2	3	4	5	6	7	8	9	10	11	##	1	2	3	4	5	6	7	8	9	10	11	12	1	2	3	4	5	6	7	8	9	10	11	12
Literature review (Background and State of the art)	■	■	■	■	■	■	■	■	■	■	■	■	■	■	■	■	■	■	■	■	■	■	■	■	■	■	■	■	■	■	■	■	■	■	■	■	■	■	■	■								
Proposal preparation	■	■	■	■	■	■	■	■	■	■	■																																					
Definition of a basic forward model with different configurations			■	■																																												
Generation of Colouration maps for the differents models							■		■																																							
Develop a reconstruction method								■																																								
Evaluation of the effect of layers in the recovery of parameters										■																																							
Writing research proposal				■	■	■	■	■	■	■																																						
Development of a more realistic model of the human head													■	■	■	■																																
Characterization of the effect of histophysiological compounds in the tissue and evaluate its contribution to																■	■	■	■	■																											
Simulation of the blood in the scalp, quantify and evaluate its optical effect																	■	■	■	■	■	■																									
Development of a reconstruction method without a priori information																					■	■	■	■	■	■	■	■																			
Inclusion of the a priori information in the reconstruction method																									■	■	■	■	■																		
Evaluation of both approaces (with and without a priori) with synthetic data generated with the forward model																												■	■	■	■																
Writing articles					■	■							■	■					■	■			■	■				■	■					■	■													
Writing thesis																		■	■	■	■	■	■	■	■	■	■	■	■	■	■	■	■	■	■	■	■	■	■	■								
Thesis defense																																					■	■										

Figure 16: Planned Schedule

32

5 Preliminary Results

The experiment performed for this proposal has the main goal to exhibit a first insight of the aforementioned hypothesis. Candid solutions for each step have been implemented aiming at achiving a first reconstruction. This, by:

- Developing a first model of the head with simple geometry and homogeneous properties

- The simulation of the gray matter oxygenation due to neural activity varying the haemoglobin concentrations.

- The generation of each spectral intensity distribution for every vector of cortical HbO_2, HHb

- The generation of a coarse colouration map.

- Use a candid reconstruct method to recover cortical HbO_2, HHb based on nearest neighbour

5.1 Forward model: image formation

5.1.1 The radiative transport model

We have chosen the Monte Carlo method as the model of radiation transport because its flexibility. Specifically we have used the implementation provided by (Wang *et al.*, 1995) which implementation's flowchart is depicted in Figure 17. Also the GPU version of (Alerstam *et al.*, 2008) was used.

5.1.2 Human Head model

A first tissue model of the adult head, inspired by the work of Okada & Delpy (2003) has been defined, consisting of the four main flat and homogeneous layers; scalp, skull, gray matter and white matter (see Figure 18). Each layer is defined by their optical properties: refraction index n, absorption coefficient μ_a, scattering coefficient μ_s, anysotropy factor g and layer thickness d.

In contrast with the model of Okada & Delpy (2003), this is defined for a wide range of the NIR light, i.e., there are specific values for every optical parameter for each wavelength in the NIR range (with 1nm resolution). All these values were collected in the literature (Bashkatov *et al.*, 2011; Choi *et al.*, 2004; Custo *et al.*, 2006; Dehaes *et al.*, 2011; Firbank *et al.*, 1993; Hueber *et al.*, 2001; Jacques, 2013; Johns *et al.*, 1998; Madsen & Wilson, 2013; Bashkatov *et al.*, 2006; Friebel *et al.*, 1999; Sandell & Zhu, 2012; Sassaroli *et al.*, 2000; Simpson *et al.*, 1998; Taddeucci *et al.*, 1996; Van Der Zee & Essenpreis, 1993; Yavari & Dam, 2005). Figure 19 shows the optical
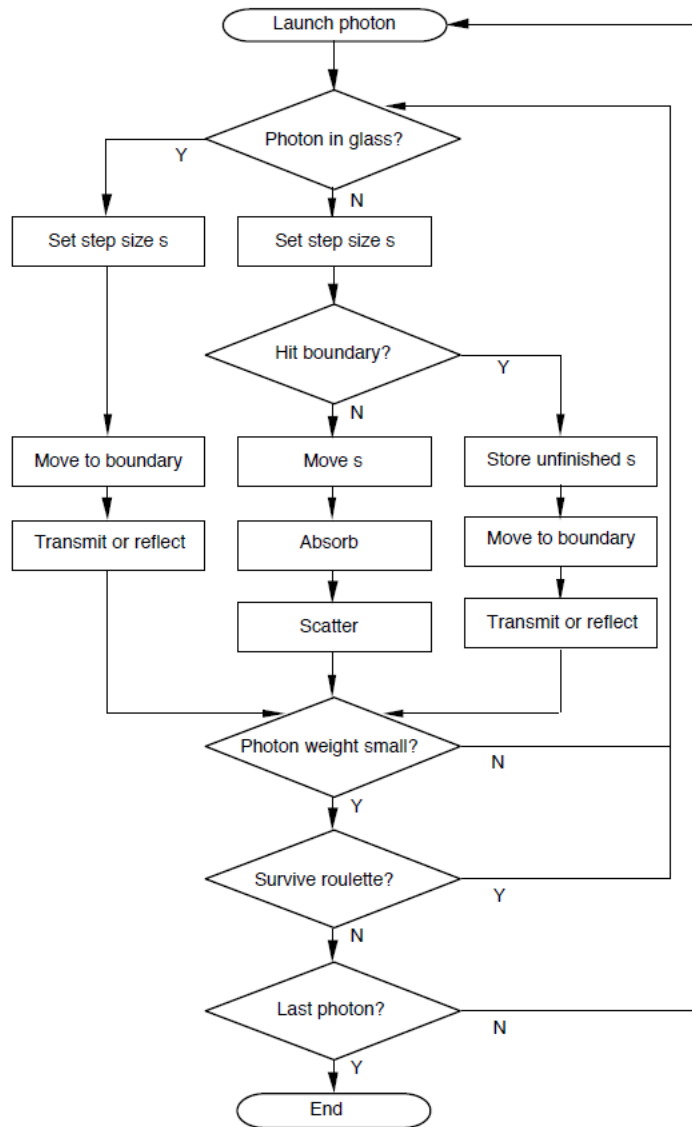
Figure 17: Flowchart of the simulator developed by Wang *et al.* (1995). The simulation is carried out launching a photon with a given start energy which is decremented by absorption through the tissue. The photon's step size and scattering direction is set by sampling over two probability density functions respectively. Photon energy is stored as absorbance, transmittance and/or reflectance.
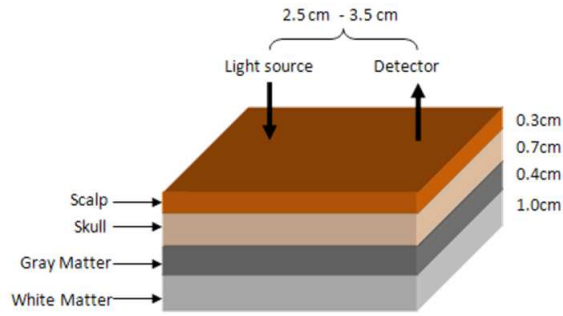
Figure 18: Human head model consisting of four main tissue layers with flat geometry

properties: absorption coefficient μ_a, scattering coefficient μ_s and anysotropy factor g for each layer in the wavelengths range from 800nm to 950nm.

5.1.3 Simulating neural activity

As the marker of neural activity is the change in concentration of HbO_2 and HHb in gray matter and hence this affect the absorption in this tissue, this effect has been simulated by altering the absorption coefficient in the gray matter in function of the concentration of both haemoglobins as described by Eq. 14.

$$\mu_a^{GM}(\lambda) = \mu_a^{GM}(\lambda) + SAC_{HbO_2}(\lambda) * C_{HbO_2} + SAC_{HHb}(\lambda) * C_{HHb} \qquad (14)$$

Where the terms SAC_{HbO_2} and SAC_{HHb} are the *specific absorption coefficient* which represent the molecular absorption of the chromophore. In this equation the resulting absorption coefficient considers: the normal absorption of the gray matter plus the absorption due to the concentration of each kind of haemoglobin. Although the light is also attenuated by scattering, this coefficient of the gray matter remains unaltered.

5.1.4 Parameters space

The parameters space was defined discretizing the physiological range of haemoglobin concentration. This data was obtained from the work of McIntosh *et al.* (2010). Which reports absolute concentrations of $HbO_2 = 25.9 \pm 3.9 \mu M$ and $HHb = 19.1 \pm 2.3 \mu M$. The parameters space consider 5 concentrations for each parameter, each one defined by $\mu \pm k\sigma$ with $k = 0, 1, 2$, resulting in 25 points in the space for every combination (parameters vector) $< HbO2, HHb >$.

5.1.5 Spectral Intensity Distribution (SID)

For each vector in the parameters space, the diffuse reflectance was computed with the forward model for every wavelength and considering models with i) 2 layers (gray and
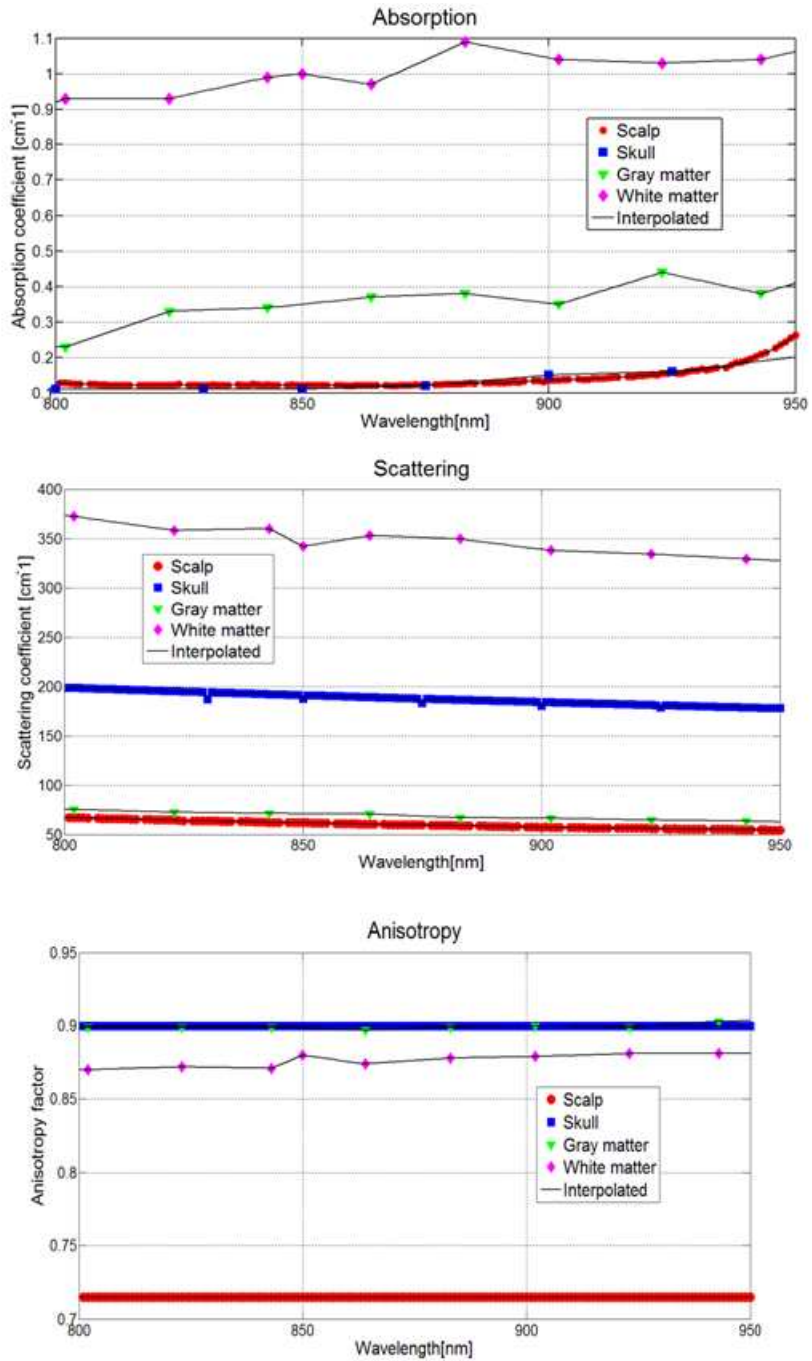
35

Figure 19: Optical properties collected in the literature used to define the model. Black line represent interpolated coefficients which was not available in literature.

white matter), ii) 3 layers (adding skull) and iii) 4 layers (adding scalp) in order to analyse the effect of each layer in the generated spectrum.

The Figure 20 shows an example of the SIDs produced for a fixed concentration of HHb and the 5 concentrations of HbO_2 for each model i),ii) and iii).

For the model of two layers it can be appreciated the clear monotonic behaviour in the measured reflectance in the whole range of wavelengths, i.e., the reflectance decrease as the concentration of HbO_2 increase.

For the models of three and four layers a more noisy spectrum is generated and in some wavelengths the lost of monotonicity (lines crossing each other) becomes obvious. This observation exemplifies the effect of superficial layers on the remitted spectrum.

5.2 Image Acquisition

5.2.1 Colouration Map

To generate the Colouration Map it is necessary the simulation of the acquisition process which is carried out by convolving each remitted spectrum with a set of filters (one for each parameter). We have chosen Gaussian filters approximating the quantum efficiency curves of an ideal sensor parametrised by wavelength center and the Half With at Half Maximum (HWHM). This Gaussian curves can be appreciated in figure 20 iii) centred in wavelengths(λ) 833nm (filter R_1)and 860nm (filter R_2). The first wavelength was chosen by findings in the state of the art as a good wavelength for fNIRS, second wavelength was selected arbitrary.

The figures 21 and 22 shows the colouration maps for the 3 and 4 layers models respectively. Each point represents a sensed value of reflectance for a given concentration of HbO_2, HHb (in the figure, markers corresponds to HHb and color HbO_2).

5.3 Reconstruction

Once the colouration map has been generated, a reconstruction task was carried out. to do this, a new observation was simulated altering the concentration of an arbitrary vector $< HbO_2, HHb >$ around a small value (trying to be more close to it than other points). This was projected on the colouration map by applying the filters previously defined. A nearest-neighbour approach was used to get the most similar point in the colouration map and since, in this experiment, the relation from the colouration map to parameters space is known, the corresponding approximated concentration can be retrieved.

This experiment was performed for the models of 3 and 4 layers. In the same figures 21, 22, a simulated point is showed and the corresponding nearest neighbour is indicated. It can be appreciated that for the 3 layers model the nearest neighbour correspond to the correct vector $< HbO_2, HHb >$. However, for the model of 4 layers, this was not correct obtained. This exhibit the insight of the noisy effect produced by the scalp layer.
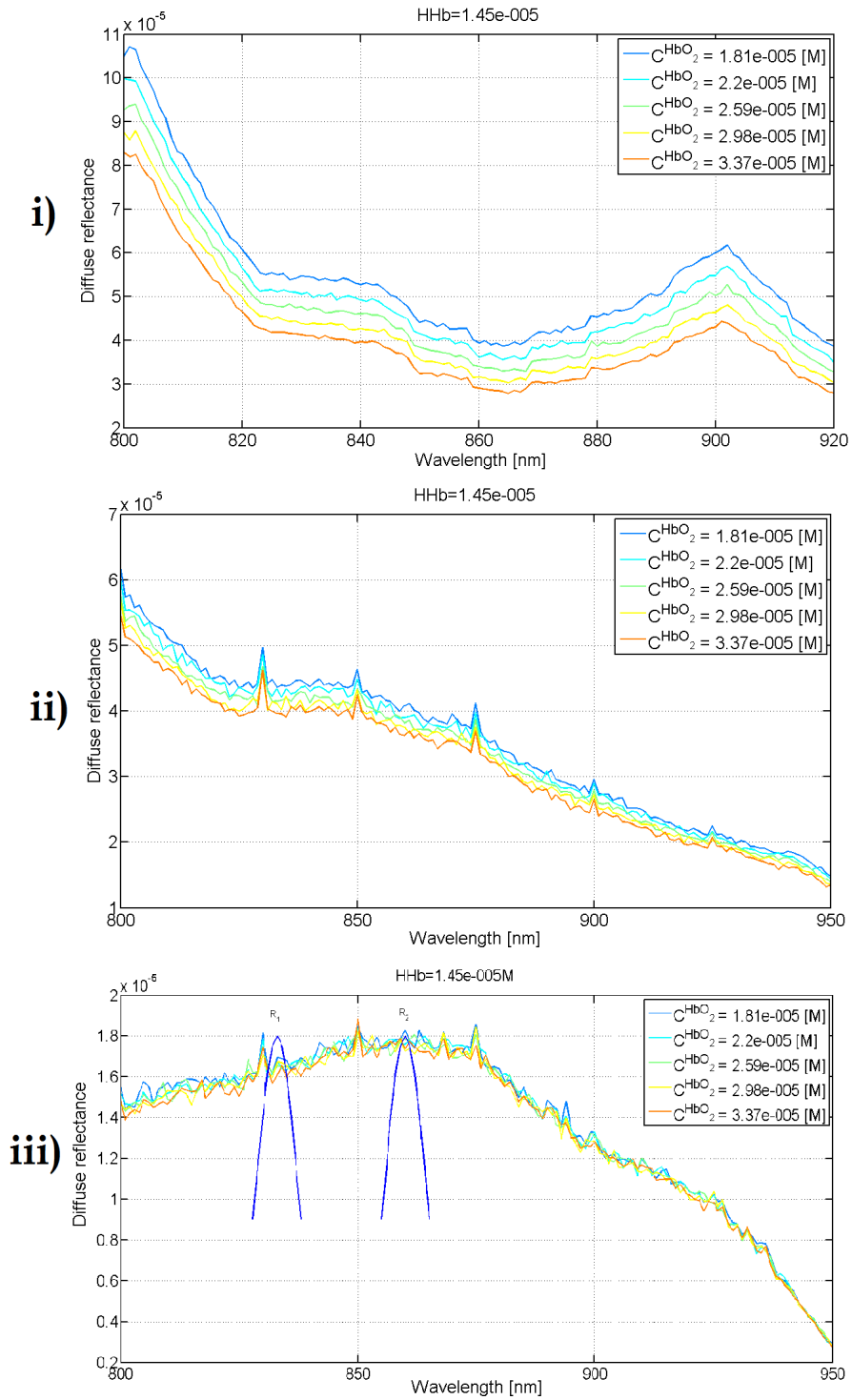
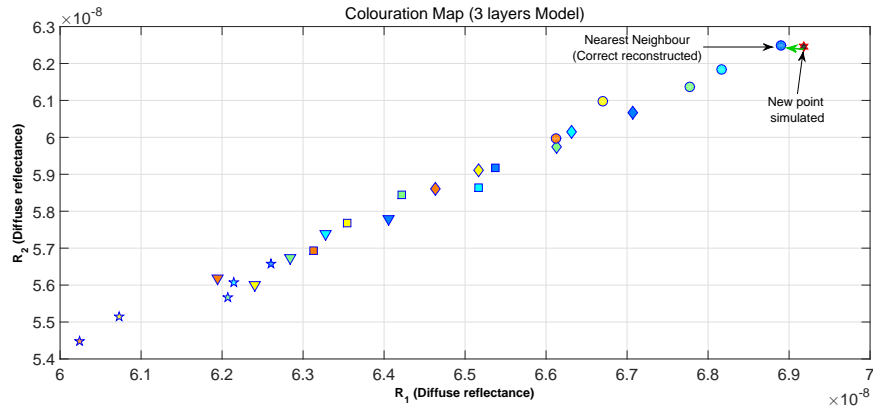Figure 20: Spectral intensity distribution.

Figure 21: Colouration map generated for the human head model consisting of 3 layers; skull, gray matter an white matter. Markers represent different levels of $HbO2$ and colour different levels of HHb. The data presents a more stable (monotonic) behaviour.

5.4 Conclusions

Despite the simplistic model and the candid reconstruction approach in this experiment, the inversion is possible and is benefited if the source of noise is avoided. When the tissue complexity increases, adding the 4th layer, this situation becomes unstable and a solution like nearest neighbour is unable to recovery correctly the parameters. Further, with a real complexity of the human head (in geometry and heterogeneity) the reconstruction problem becomes aggravated. A necessity to do more realistic models of the human head in whom be possible approximate diffuse reflectance with light propagation models is apparent. On the other hand, still with a more realistic head model or more precise light transport model the reconstruction keeps ill-posed because of the reduced dimensionality from the parameters space to the discrete image space. Thus, the only way to deal with the ill-posed inverse problem is through the computational solutions that can avoid the artefacts that prevent inversion.

5.4.1 Publications

As part of the work developed during the preparation of this research proposal the following work has been published:

- **Javier Herrera-Vega**, Karla Janeth Sánchez-Pérez, Luis Enrique Sucar, Carlos G. Treviño-Palacios, and Felipe Orihuela-Espina, "Understanding Signal-to-Noise ratio for image reconstruction in optical topography", in fNIRS2014, Montreal, Canada, October 10-12, 2014.

- Cuervo-Soto, Bibiana; **Herrera-Vega, Javier**; Garcés-Báez, Alfonso; Sucar, Luis Enrique; Treviño-Palacios, Carlos G.; Orihuela-Espina, Felipe, Facilitating tissue
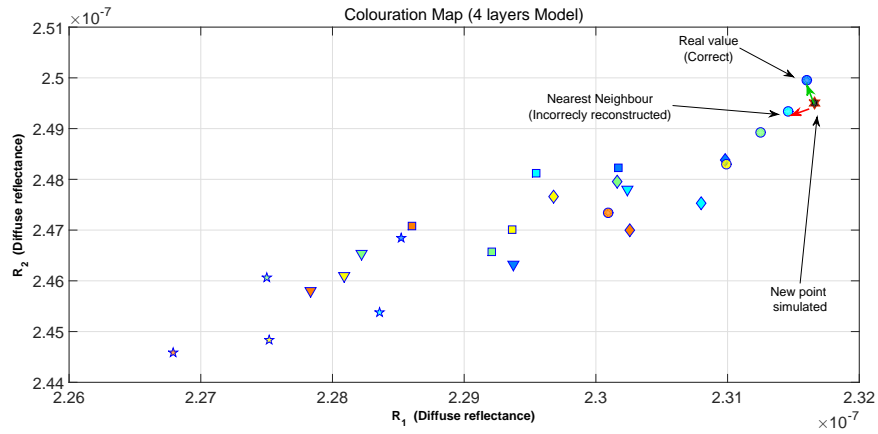
Figure 22: Colouration map generated for the human head model consisting of 4 layers; scalp,skull, gray matter an white matter. In this case the reconstruction failed to identify the correct solution.

specification and complex sensing geometries in Monte Carlo radiation transport simulations-application to functional Near Infrared Spectroscopy (fNIRS), XVI Reunion de Neuroimagen CIMAT, Guanajuato, Mexico, October 17, 2014.

6   Glossary

Diffuse light The light in which its rays travel at different angles

Photodetector Sensor of light or other electromagnetic energy

Neuroimaging The use of various techniques to either directly or indirectly image the structure, function/pharmacology of the nervous system.

Spectroscopy The study of the interaction between matter and radiated energy.

Haemodynamic In the context of neurobiology consists of the rapid delivery of blood to active neuronal tissues.

Haemoglobin species Refers to the oxyhaemoglobin and deoxyhaemoglobin

Histophysiology Relate with the structure and function of tissues

Neurovascular coupling The relationship between local neural activity and subsequent changes in cerebral blood flow.

Light extinction The term refers to the light attenuation by absorption and scattering.

Optical properties The refractive index, absorption, scattering and anysotropy coefficients dependent of the tissue and the wavelength.

References

Erik Alerstam, Tomas Svensson, & Stefan Andersson-Engels. Parallel computing with graphics processing units for high-speed monte carlo simulation of photon migration. *Journal of Biomedical Optics*, 13(6), December 2008.

S. R. Arridge & J. C. Hebden. Optical imaging in medicine: Ii. modelling and reconstruction. *Phys Med Biol.*, 42:841–853, May 1997.

Simon Arridge & M. Schweiger. A gradient-based optimisation scheme for optical tomography. *Opt. Express*, páginas 213–226, 1998.

Simon R. Arridge. Methods in diffuse optical imaging. *Philosophical Transactions of The Royal Society A*, 369:4558–4576, 2011.

Simon R Arridge & John C Schotland. Optical tomography: forward and inverse problems. *Inverse Problems*, 25, 2009.

Sylvain Baillet & Line Garnero. A bayesian approach to introducing anatomo-functional priors in the eeg/meg inverse problem. *IEEE Transactions on Biomedical Engineering*, 44(5):374–385, May 1997.

Akke Bakker, Brianne Smith, Philip Ainslie, & Kurt Smith. Near-infrared spectroscopy. *Applied Aspects of Ultrasonography in Humans*, 2012.

Alexey N. Bashkatov, Elina a. Genina, Vyacheslav I. Kochubey, & Valery V. Tuchin. Optical properties of human cranial bone in the spectral range from 800 to 2000 nm. *Proc. SPIE 6163, Saratov Fall Meet. 2005 Opt. Technol. Biophys. Med. VII*, 6163: 616310–616310–11, August 2006.

Alexey N. Bashkatov, Elina a. Genina, & Valery V. Tuchin. Optical properties of skin, subcutaneous, and muscle tissues: a review. *J. Innov. Opt. Health Sci.*, 04(01):9–38, January 2011. ISSN 1793-5458.

Mark F. Bear, Barry Connors, & Michael Paradiso. *Neuroscience: Exploring the Brain.* Lippincott Williams & Wilkins, third edición, February 2006. ISBN 0781760038.

David A. Boas, Clare E. Elwell, Marco Ferrari, & Gentaro Taga. Twenty years of functional near-infrared spectroscopy: introduction for the special issue. *Neuroimage*, 85 Pt 1:1–5, Jan 2014.

David A. Boas, T. Gaudette, Gary Strangman, Xuefeng Cheng, John J. A. Marota, & Joseph B. Mandeville. The accuracy of near infrared spectroscopy and imaging during focal changes in cerebral hemodynamics. *NeuroImage*, 2011.

Gilberto Branco. *The develpment and evaluation of head probes for optical imaging of the infant head.* PhD thesis, University College London, 2007.

JeeHyun Choi, Martin Wolf, Vladislav Toronov, Ursula Wolf, Chiara Polzonetti, Dennis Hueber, Larisa P Safonova, Rajarsi Gupta, Antonios Michalos, William Mantulin, & Enrico Gratton. Noninvasive determination of the optical properties of adult brain: near-infrared spectroscopy approach. *J. Biomed. Opt.*, 9(1):221–9, 2004. ISSN 1083-3668.

Ela Claridge, Symon Cotton, Per Hall, & Marc Moncrieff. From colour to tissue histology: Physics based interpretation of images of pigmented skin lesions. In Takeyoshi Dohi & Ron Kikinis, editors, *Medical Image Computing and Computer-Assisted Intervention MICCAI 2002*, volume 2488 of *Lecture Notes in Computer Science*, páginas 730–738. Springer Berlin Heidelberg, 2002. ISBN 978-3-540-44224-0. doi: 10.1007/3-540-45786-0_90.

Ela Claridge & Dzena Hidović-Rowe. Model based inversion for deriving maps of histological parameters characteristics of cancer from ex-vivo mutispectral images of the colon. *IEEE Transactions on Medical Imaging*, 33(4):822–835, April 2014.

Anna Custo, William M. III Wells, Alex H. Barnett, Elizabeth M. C. Hillman, & David A. Boas. Effective scattering coefficient of the cerebral spinal fluid in adult head models for diffuse optical imaging. *Applied Optics*, 45(9):4747 – 4755, July 2006.

Mathieu Dehaes, P. Ellen Grant, Danielle D. Sliva, Nadege Roche-Labarbe, Rudolph Pienaar, David A. Boas, Maria Angela Franceschini, & Juliette Selb. Evaluation of the accuracy of brain optical properties estimation at different ages using the frequency-domain multi-distance method. *Proc. SPIE*, 7892:789203–789203–12, February 2011.

Hamid Dehghani, Subhadra Srinivasan, Brian W. Pogue, & Adam Gibson. Numerical modelling and image reconstruction in diffuse optical tomography. *Philos Trans A Math Phys Eng Sci*, 367:3073–3093, Aug 2009a.

Hamid Dehghani, Brian R. White, Benjamin W Zeff, Andrew Tizzard, & Joseph P. Culver. Deep sensitivity and image reconstruction analysis of dense imaging arrays for mapping brain function with diffuse optical tomography. *Commun Numer Methods Eng*, 48:D137–D143, April 2009b.

David T. Delpy, Mark Cope, & Pieter van der Zee. Estimation of optical path length through tissue from direct time of flight measurement. *Physic in Medicine and Biology*, 33(12):1433–1442, 1988.

Harold Ellis & Vishy Mahadevan. The surgical anatomy of thescalp. *Surgery - Oxford International Edition*, 2013.

M Firbank, M Hiraoka, M Essenpreis, & D T Delpy. Measurement of the optical properties of the skull in the wavelength range 650-950 nm. *Phys. Med. Biol.*, 38(4):503–510, 1993.

Moritz Friebel, Klaus Do, Andreas Hahn, Gerhard Mu, D Berlin, Laser Medizin, & Freie Universita. Optical properties of circulating human blood in the wavelength range 400 - 2500 nm. *J. Biomed. Opt.*, 4(1):36–46, 1999.

Jacques Hadamard. Sur les problèmes aux dérivées partielles et leur signification physique. *Princeton University Bulletin*, páginas 49–52, 1902.

Florian B. Haeussinger, Sebastian Heinzel, Tim Hahn, Martin Schecklmann, Ann-Christine Ehlis, & Andreas J. Fallgatter. Simulation of near-infrared light absorption considering individual head and prefrontal cortex anatomy: Implications for optical neuroimaging. *PLoS ONE*, 6(10), October 2011.

D M Hueber, M A Franceschini, H Y Ma, Q Zhang, J R Ballesteros, S Fantini, D Wallace, V Ntziachristos, & B Chance. Non-invasive and quantitative near-infrared haemoglobin spectrometry in the piglet brain during hypoxic stress, using a frequency-domain multidistance instrument. *Phys. Med. Biol.*, 46(1):41–62, 2001.

Steven L Jacques. Corrigendum: Optical properties of biological tissues: a review. *Phys. Med. Biol.*, 58(14):5007–5008, July 2013. ISSN 0031-9155.

Huabei Jiang, Keith D. Paulsen, Ulf L. Osterberg, Brian W. Pogue, & Michael S. Patterson. Optical image reconstruction using frequency-domain data: simulations and experiments-. *J. Opt. Soc. Am. A*, 13:253–266, Feb 1996.

Maureen Johns, Cole Giller, & Hanli Liu. Computational and in vivo investigation of optical reflectance from human brain to assist neurosurgery. *J. Biomed. Opt.*, 3(4): 437–445, 1998.

E. J Kansa. Multiquadrics ? a scattered data approximation scheme with applications to computational fluid dynamics ii. *Computers Math. Appl.*, 19(8):147–161, 1990.

Evgeniya Kirilina, Na Yu, Alexander Jelzow, Heidrun Wabnitz, Arthur M Jacobs, & Ilias Tachtsidis. Identifying and quantifying main components of physiological noise in functional near infrared spectroscopy on the prefrontal cortex. *Frontiers in Neuroscience*, 2013.

S Kohno, I Miyai, A Seiyama, I Oda, A Ishikawa, S Tsuneishi, T Amita, & K Shimizu. Removal of the skin blood flow artifact in functional near-infrared spectroscopic imaging data through independent component analysis. *Journal of biomedical optics*, 2007.

Steven Lemma, Benjamin Blankertza, & Thorsten Dickhausa Klaus-Robert Müllera. Introduction to machine learning for brain imaging. *NeuroImage*, 56(2):387–399, May 2011.

Steen J Madsen & Brian C Wilson. *Optical Methods and Instrumentation in Brain Imaging and Therapy.* Springer New York, New York, NY, 2013. ISBN 978-1-4614-4977-5.

Chris Martin. Contributions and complexities from the use of in-vivo animal models to improve understanding of human neuroimaging signals. *Frontiers in Neuroscience*, 8 (211), 2014.

M. A. McIntosh, Uma Shahani, & D. L. McCulloch. Absolute quantification of oxygenated hemoglobin within the visual cortex with functional near infrared spectroscopy (fnirs). *Invest Ophthalmol Vis Sci.*, 51:4856–460., Sep 2010.

MichaelI. Mishchenko. Radiative transfer theory: From maxwell's equations to practical applications. In BartA. van Tiggelen & SergeyE. Skipetrov, editors, *Wave Scattering in Complex Media: From Theory to Applications*, volume 107 of *NATO Science Series*, páginas 366–414. Springer Netherlands, 2003. ISBN 978-1-4020-1394-2.

J. Antonio Muñoz-Gómez, Pedro González-Casanova, & Gustavo Rodríguez-Gómez. Meshfree methods for evolutionary partial differential equations. Technical Report CCC-05-001, Instituto Nacional de Astrofísica, Óptivca y Electrónica, January 2005.

E. Okada & D. T. Delpy. Near-infrared light propagation in an adult head model. i. modeling of low-level scattering in the cerebrospinal fluid layer. *Appl. Opt.*, 42:2906–214., Jun 2003.

Eiji Okada. *Application of Near Infrared Spectroscopy in Biomedicine*, chapter Photon Migration in NIRS Brain Imaging, páginas 37–58. Springer, 2013.

F. Orihuela-Espina, D. R. Leff, D. R. C. James, A. W. Darzi, & G. Z. Yang. Quality control and assurance in functional near infrared spectroscopy (fnirs) experimentation. *Phys Med Biol*, 55:3701–3724, Jul 2010.

Felipe Orihuela-Espina. *Modelling and verification of the diffuse reflectance of the ocular fundus.* PhD thesis, Department of Computer Science, University of Birmingham, August 2005.

Sundeep Patel, Takusige Katura, Atsushi Maki, & Ilias Tachtsidis. *Oxygen Transport to Tissue XXXII*, volume 701 of *Advances in Experimental Medicine and Biology*, chapter Quantification of Systemic Interference in Optical Topography Data during Frontal Lobe and Motor Cortex Activation: An Independent Component Analysis, páginas 45–51. Springer US, 2011.

Jaya Prakash, Venkittarayan Chandrasekharan, Vishwajith Upendra, & Phaneendra K. Yalavarthy. Accelerating frequency-domain diffuse optical tomographic image reconstruction using graphics processing units. *J Biomed Opt*, 15, Jan 2010.

S.J. Preece & E. Claridge. Spectral filter optimization for the recovery of parameters which describe human skin. *IEEE Transactions on Pattern Analysis and Machine Intelligence*, 2004.

Web resource:. Layers of the scalp, 2015a. URL `www.studyblue.com`.

Web resource:. Light penetration in brain tissue using imagent., 2015b. URL `http://www.iss.com/biomedical/instruments/imagent.html`.

Web resource:. A section of the head showing the protective layers (meninges and scalp) of the brain, January 2015c. URL `http://m.inmagine.com/`.

Julia L Sandell & Timothy C Zhu. A review of in-vivo optical properties of human tissues and its impact on pdt. *J Biophotonics*, 4:773–787, 2012.

Angelo Sassaroli, Fabrizio Maertelli, Yukari Tanikawa, Kenji Tanaka, Ryuichiro Araki, Yoichi Onodera, & Yukio Yamada. Time-resolved measurements of in vivo optical properties of piglet brain. *Opt. Rev.*, 7(5):420–425, 2000.

Felix Scholkmann, Stefan Kleiser, Andreas Jaakko Metz, Raphael Zimmermann, Juan Mata Pavia, Ursula Wolf, & Martin Wolf. A review on continuous wave functional near-infrared spectroscopy and imaging instrumentation and methodology. *NeuroImage*, 2014.

Rebecca C. Simpson, Matthias Kohl, Matthias Essenpreis, & Mark Cope. Near-infrared optical properties of ex vivo human skin and subcutaneous tissues measured using the Monte Carlo inversion technique. *Phys. Med. Biol.*, 43:2465–2478, 1998.

Olaf Sporns. Networks of the brain: Quantitative analysis and modeling, 2010.

Gary Strangman, David A. Boas, & P. Jeffrey Sutton. Non-invasive neuroimaging using near-infrared light. *Biol Psychiatry.*, 52:679, Oct 2002.

Ilias Tachtsidis, Peck H. Koh, Charlotte Stubbs, & Clare E. Elwell. Functional optical topography analysis using statistical parametric mapping (spm) methodology with and without physiological confounds. *Advances in Experimental Medicine and Biology*, 662: 237–243, 2010.

Adriana Taddeucci, Fabrizio Martelli, Marco Barilli, Marco Ferrari, & Giovanni Zaccanti. Optical properties of brain tissue. *J. Biomed. Opt.*, 1(1):117–123, 1996.

Toshimitsu Takahashi, Yoriko Takikawa, Reiko Kawagoe, Satoshi Shibuya, Takayuki Iwano, & Shigeru Kitazawa. Influence of skin blood flow on near-infrared spectroscopy signals measured on the forehead during a verbal fluency task. *Neuroimage*, 57(3):991–1002, 2011.

K. Uludag, Kohl M, J. Steinbrink, H. Obrig, & A. Villringer. Cross talk in the lambert-beer calculation for near-infrared wavelengths estimated by monte carlo simulations. *Journal of Biomedical Optics*, 7:51–9., 2002.

Kâmil Uludag, Jens Steinbrink, Arno Villringer, & Hellmuth Obrig. Separability and cross talk: optimizing dual wavelength combinations for near-infrared spectroscopy of the adult head. *NeuroImage*, 22(2):583–589, June 2004.

Pieter Van Der Zee & Matthias Essenpreis. Optical properties of brain tissue. *Proc. SPIE 1888, Phot. Migr. Imaging Random Media Tissues*, páginas 454–465, 1993.

Arno Villringer & Britton Chance. Non-invasive optical spectroscopy and imaging of human brain function. *Trends Neurosci.*, 20:435–442, 1997.

Lihong Wang, Steven L. Jacques, & Liqiong Zheng. Mcml—monte carlo modeling of light transport in multi-layered tissues. *Computer Methods and Programs in Biomedicine*, 47:131–146, Jun 1995.

Prof. Dr. Yanfei Wang, Prof. Dr. Changchun Yang, & Prof. Dr. Anatoly G. Yagola, editors. *Optimization and Regularization for Computational Inverse Problems and Applications.* Springer Berlin Heidelberg, 2011.

N Yavari & J S Dam. In vitro measurements of optical properties of porcine brain using a novel compact device. *Med. Biol. Eng. Comput.*, 43:658–666, 2005.

Wenwu Zhu, Yao Wang, Yuqi Yao, Jenghwa Chang, Harry L. Graber, & Randall L. Barbour. Iterative total least-squares image reconstruction algorithm for optical tomography by the conjugate gradient method. *Journal of the Optical Society of America*, 14(4):799–807, 1997.